UNIVERSITY OF NAPLES FEDERICO II

DEPARTMENT OF PHARMACY

PhD course in Pharmaceutical Sciences

PHARMACOLOGICAL EFFECTS OF PALMITOYLETHANOLAMIDE, AN ENDOGENOUS N-ACYLETHANOLAMINES, IN MODULATION OF MITOCHONDRIAL AND METABOLIC FUNCTION

PhD student

CHIARA ANNUNZIATA

Coordinator
Prof.
MARIA VALERIA D'AURIA

Tutor
Prof.
ROSARIA MELI

XXXII (2017-2020)

SUMMARY

Abstract

Liver and adipose tissue are closely related, and their mutual connection directly affects the whole-body energy homeostasis, being the key regulators of metabolic function. Not surprisingly, non-alcoholic fatty liver disease (NAFLD) and obesity usually arise in the same individual together with other metabolic abnormalities such as hypertension, atherosclerosis and hyperlipidemia and lead to the onset of a serious clinical condition known as metabolic syndrome.

Palmitoylethanolamide (PEA) is an endogenous Autacoid Local Injury Antagonist amides (ALIAmide), biosynthesized on demand to maintain homeostasis in cell when it is insulted by stress-conditions. Pharmacological properties of PEA include analgesic, anti-inflammatory and neuroprotective effect. Over the years, PEA has been recognized as a potent agonist of peroxisome proliferator-activated receptor (PPAR)-α, whose activation mediates the anti-inflammatory and analgesic effects evoked by this lipid mediator.

PPAR-α, as nuclear transcription factor, controls the complex network and pathways underlying cellular energy requirements and lipid and glucose metabolism.

The aim of the study was focused on immunometabolic and pharmacological effects of PEA in a mouse model of obesity and correlated disease (i.e. non-alcoholic fatty liver disease, NAFLD) due to overnutrition induced by the assumption of a high fat diet (HFD).

Long-term administration of PEA (30mg/kg/*die*) limited hepatic metabolic inflexibility in obese mice through the activation of 5' adenosine

monophosphate-activated protein kinase (AMPK) pathway, the signaling cascade that provides metabolic regulation of the cells according with nutrient status. PEA enhanced mitochondrial oxidative capacity and energy efficiency in hepatic isolated mitochondria. *In vitro* evidence addressed the direct involvement of AMPK in PEA-induced adaptative setting. PEA treatment ameliorated hepatocytes metabolism, improving mitochondrial bioenergetics and recovering mitochondrial dysfunction in insulin-resistant cells. In the latter part of the study, is described the effect of PEA on brown and white adipose tissue (BAT and WAT, respectively) activation and function. PEA promoted the recovery of BAT morphological features activation and allowed the adaptative thermogenesis in response to overfeeding. Furthermore, in subcutaneous WAT, this lipid mediator reverted adipose leptin resistance and induced tissue plasticity stimulating fat metabolism in obese mice.

In light of the obtained data, PEA can be considered a therapeutic tool to improve metabolic flexibility impaired by obesity. PEA limits metabolic impairment, counteracting lipid accumulation in liver and adipose tissue, the main tissues involved in energy homeostasis and metabolism. The beneficial effects of PEA may be the result of multiple direct and indirect converging mechanisms: the improvement of mitochondrial efficiency, its well- known anti-inflammatory effects, and its new determined capability to modulate adipose tissue plasticity.

Introduction

Metabolic flexibility is defined as the ability of several tissues (i.e, liver, adipose tissue, skeletal muscle, and heart) to adapt metabolism and manage nutrient availability, switching from fatty acid oxidation (FAO) during fasting to glucose metabolism during the fed state. The impairment of these mechanisms has been associated with obesity and type 2 diabetes, but it is still unknown whether this detrimental condition is cause or a consequence of these pathologies (Smith et al. 2018). High fat feeding promotes an increased level of FAO rate in lean individual, that is a result of an adequate metabolic flexibility, and leads to the transcriptional regulation of gene involved in fatty acid transport and oxidation (Battaglia et al. 2012). Inversely, the onset of inflexibility is due to an imbalance between energy consumption and expenditure and results in ectopic accumulation of lipid and in the development of insulin resistance (IR) (Morino et al. 2006).

In the liver, the impairment of FAO provokes the release of toxic lipid intermediates, altering insulin signaling pathway and triggering oxidative stress and subsequent mitochondrial dysfunction, a crucial feature of metabolic disorders (Begriche et al. 2013, Khan et al. 2019). Indeed, mitochondria represent the powerhouse of the cells, provide bioenergetic reaction and adapt cellular metabolism to nutrient supply and energy demand, changing their morphology and architecture (Obre and Rossignol 2015, Theurey and Rieusset 2017).

In non-alcoholic fatty liver disease (NAFLD), chronic toxic lipid overload causes the activation of inflammatory pathways, also resulting in an altered hormonal tone (Meli et al. 2014). Indeed, besides collecting

nutrients, portal blood drains different mediators released from gut and visceral adipose tissue (Konrad and Wueest 2014). Therefore, hepatic metabolism is directly affected not only by nutrients assumed from the diet but also by the secretory profile of visceral fat, highlighting the endocrine and immune interactions in NAFLD-related diseases (Meli et al. 2014).

Peroxisome proliferator-activated receptors (PPARs) are ligand-inducible transcription factors, and despite their common structural homology and activity, are characterized by distinct and tissue-specific pattern of activity (Bougarne et al. 2018). Among these, PPAR-α was the first identified subtype and is the main nuclear transcription factor able to exert positive and/or negative control over the expression of a wide range of metabolic and inflammatory genes (Bensinger and Tontonoz 2008). PPAR-α activation also mediates the interplay between liver and adipose tissue in regulating whole-body energy metabolism. Although PPAR-γ is a master adipogenic transcription factor of adipocytes differentiation program (Poulos et al. 2016), PPAR-α activation is a crucial step in adipose tissue plasticity, as demonstrated by its obligatory role in leptin-mediated lipolytic effect (Lee et al. 2002, Tsuchida et al. 2005). Indeed, acting on the transcriptional regulation of gene encoding mitochondrial enzymes for fatty acid catabolism, PPAR-α modulates the release of fatty acids, the main fuel for the thermogenic activity (Barbera et al. 2001, Lee et al. 2018) and promptly stimulates gene pathway involved in brown adipose tissue (BAT) development (Barbera et al. 2001, Hondares et al. 2011). After the identification of BAT in adult human (Cypess et al. 2009), several approaches have been proposed to dissipate excess of energy. Palmitoylethanolamide (PEA) is an endogenous bioactive compound and a PPAR-

α ligand with a well-known anti-inflammatory and analgesic properties (Mattace Raso et al. 2014).

Recently, a cohort study investigated the effect of dysmetabolism on PEA and other congener circulating levels, whose concentration and ratio were profoundly altered in obese patients (Fanelli et al. 2018). Moreover, experimental findings demonstrate that PEA was able to manage energy balance in a rat model of mild obesity and in diabetic rats (Izzo et al. 2010, Mattace Raso et al. 2014), highlighting the metabolic features of PEA and its pharmacological potential in metabolic diseases.

1. Pharmacology of PEA

1.1 An ancient discover and a novel therapeutic opportunity

In 1993, the Nobel Prize Rita Levi-Montalcini identified a protective anti-inflammatory role of the endogenous autacoid compounds N-acylethanolamines (NAEs) (Aloe et al. 1993). Her studies provided new insight into the mechanism by which the autacoid molecules control the mast cells behavior during inflammation. These findings gave rise to numerous other studies aiming at investigating the role of these molecules in health and disease. N-acylethanolamines are a family of endogenous bioactive lipids synthesized "on demand" from membrane glycerophospholipids (Tsuboi et al. 2018), involved in inflammation, pain, food intake, and neuronal control (Mattace Raso et al. 2014). Despite belonging to the same family of molecules and sharing biosynthetic and metabolic pathways, each NAE owns its molecular target and exerts diverse effects (Alhouayek and Muccioli 2014). The endocannabinoid N-arachidonoylethanolamine (or anandamide, AEA) and 2-arachidonoyl-glicerol (2-AG) classically bind CB1 and CB2 receptors (Devane et al. 1992, Mechoulam et al. 1995), but also the transient receptor potential vanilloid (TRPV)1 receptor (Zygmunt et al. 1999) (***Fig.1.1.1***). N-oleoylethanolamine (OEA) is a ligand of G protein-coupled receptors (GPCR)119 (Lauffer et al. 2009), TRPV1 (Ahern 2003) and PPAR-α (Guzmán et al. 2004) (for review see Bottemanne et al. (2018)). Even if PEA was isolated more than 50 years ago (Long and Martin 1956, Bachur et al. 1965), it was later identified as PPAR-α agonist (Lo Verme et al. 2005) and a ligand of the orphan G protein-

coupled receptor (GPR)55 (Ryberg et al. 2007). Over the years, PEA has been shown to exert a plethora of pharmacological effects, mainly related to its anti-inflammatory and neuroprotective properties (Mattace Raso et al. 2014). Nowadays the clinical significance of PEA in pain control is well recognized, but several new directions need to be explored to fully understand its effect in other pathological conditions.

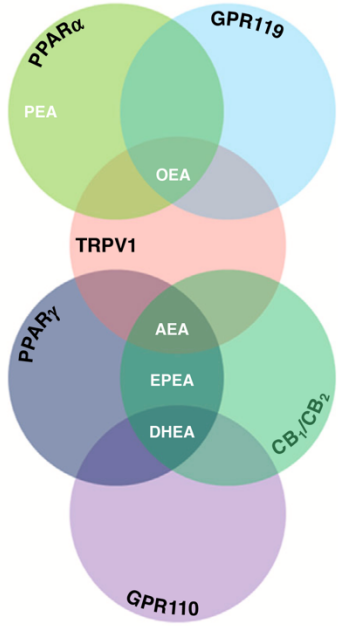

Figure 1.1.1 Simplified overview of NAEs molecular target (from Bottemanne et al, Drug Discov Today 2018).

1.2 Metabolism and biological activities of PEA

NAEs have a common chemical scaffold, an ethanolamine of acyl chain, but they can be distinguished by the length of carboxylic chain and the number of unsaturation.

In response of various stimuli, NAEs are produced from N-acylated ethanolamine phospholipids (Tsuboi et al. 2018). As shown in ***Fig. 1.2.1*** the first reaction of the canonical biosynthetic route (1) produces a N-acyl-phosphatidylethanolamine (NAPE), transferring an acyl-group (palmitic acid) from phosphatidylcholine (PC) to phosphatidylethanolamine (PE); subsequently NAPE (2) is hydrolyzed in NAEs by a specific phospholipase D (PLD)-type enzyme (NAPE-PLD) (Ueda et al. 2013). Beyond the classical one step pathway, a multi-step NAPE-PLD independent reaction was identified in mammals (Tsuboi et al. 2011).

NAEs are degraded in free fatty acids and ethanolamine by fatty acid amide hydrolase (FAAH) (3), located in the endoplasmic reticulum and characterized by a high affinity for AEA (Cravatt et al. 1996). On the other hand, N-Acylethanolamine-hydrolyzing acid amidase (NAAA) is a lysosomal enzyme mostly abundant in macrophages, which preferentially hydrolyzes PEA (Ueda et al. 2013). Because of the enzyme localization and affinity, NAAA inhibitors could be a useful and specific anti-inflammatory tool. Many findings showed that PEA metabolism was altered during inflammation, worsening some pathological processes. Indeed, in *in vivo* and *in vitro* models of inflammation (i.e. carrageenan- or lipopolysaccharide-induced inflammation), the decreased PEA levels exacerbated the inflammatory response (Endocannabinoid Research et al. 2010, Zhu et al. 2011, Izzo et al. 2012) and were re-established by the anti-inflammatory treatments (Jhaveri et al. 2008). All these findings prompted the scientific community in developing several NAAA inhibitors and validating their pharmacological activities in pain, inflammation and cancer (Bottemanne et al. 2018). In the early of the century, the structural similarity among NAEs placed PEA as a cannabinoid receptor (CB)2 agonist (Facci et

al. 1995). Moreover, the pharmacological blockade of CB2 receptor attenuated some of PEA anti-inflammatory effects (Calignano et al. 1998, Calignano et al. 2001). Conversely, the anti-peristaltic effect of PEA was not blunted in presence of SR144528, the antagonist of CB2 receptor (Capasso et al. 2001).

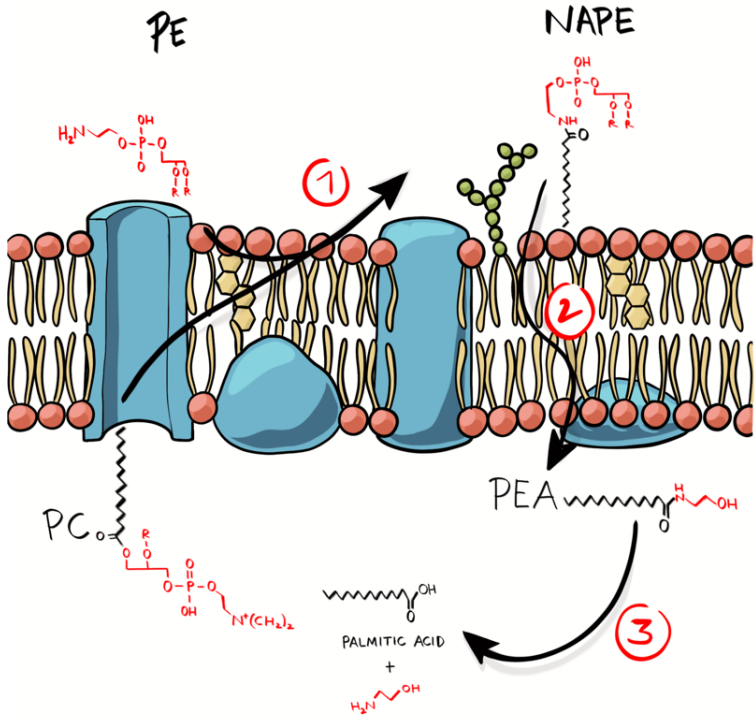

Figure 1.2.1 Canonical biosynthetic route and degradation of PEA

Latter studies clarified that PEA has poor affinity for CB2 receptor (Sugiura et al. 2000); on the contrary, PEA more specifically bind the nuclear PPAR-α receptor, even at low concentrations (***Fig 1.3, C***). PEA activates PPAR-α with a half-maximal effective concentration (EC_{50}) of 3 μM and its anti-inflammatory effects were absent in PPAR-α null mice (Lo Verme et al. 2005). Binding PPAR-α, PEA induce not only a fast reduction but also a

reinforcing delayed effect on neuronal firing. A first PPAR-α dependent non-genomic mechanism leads to an increase gating of calcium-activated intermediate (IKCa) and big-conductance potassium (BKCa) potassium channels, responsible of a fast reduction of neuronal firing (**Fig 1.3, C**) (Mattace Raso et al. 2014).

In acute or persistent pain mice model, Sasso et al. (2012) demonstrated that PEA induced PPARα activation increased Cl^- fluxes via a positive allosteric activation of aminobutyric acid (GABA)-A receptors. Indeed, PEA promoted the increased expression of steroidogenic acute regulatory protein (StAR) and cytochrome P450 side-chain cleavage (CYP450scc), enhancing cholesterol flux into the mitochondria, the metabolic conversion into pregnanolone and the subsequent increase of allopregnanolone levels (**Fig 1.3.1, C**) (Locci and Pinna 2019).

Moreover, the anti-inflammatory effects of PEA seem to be correlated with PPAR-α capability in preventing the nuclear translocation of NF-kB and repressing the expression of pro-inflammatory proteins (i.e. TNF-a, IL-1b), dampening the transcription of pro-inflammatory gene (**Fig 1.3.1, C**) (Mattace Raso et al. 2014). Interestingly, it has also been reported a direct interaction of PEA with G protein-coupled receptor (GPR)55 and 119 (Godlewski et al. 2009).

This intriguing pharmacological scenario leads to the "entourage effect" theory, whereby PEA exerts other indirect-receptor mediated effects (Mattace Raso et al. 2014). Indeed, PEA could increase AEA and thus indirectly activates CB receptors through a competitive inhibition of FAAH (Petrosino and Di Marzo 2017) and/or via the allosteric activity on transient receptor potential channel type V1 (TRPV1), also known as the vanilloid receptor type 1 (De Petrocellis et al. 2004, Ho et al. 2008). Moreover, it has

been shown that PEA was able to increase AEA- and 2-AG-mediated activation or desensitization of TRPV1 (De Petrocellis et al. 2001, Petrosino et al. 2016).

These diverse results and multiple PEA mechanism of actions suggest that it can carry out its pharmacological effects via several and/or convergent mechanisms, depending on the different etiopathogenetic aspects involved in the several diseases in which PEA exerts its pharmacological efficacy.

In the figure (**Fig.1.3.1, A-B**) the direct and indirect mechanisms of action of PEA are shown.

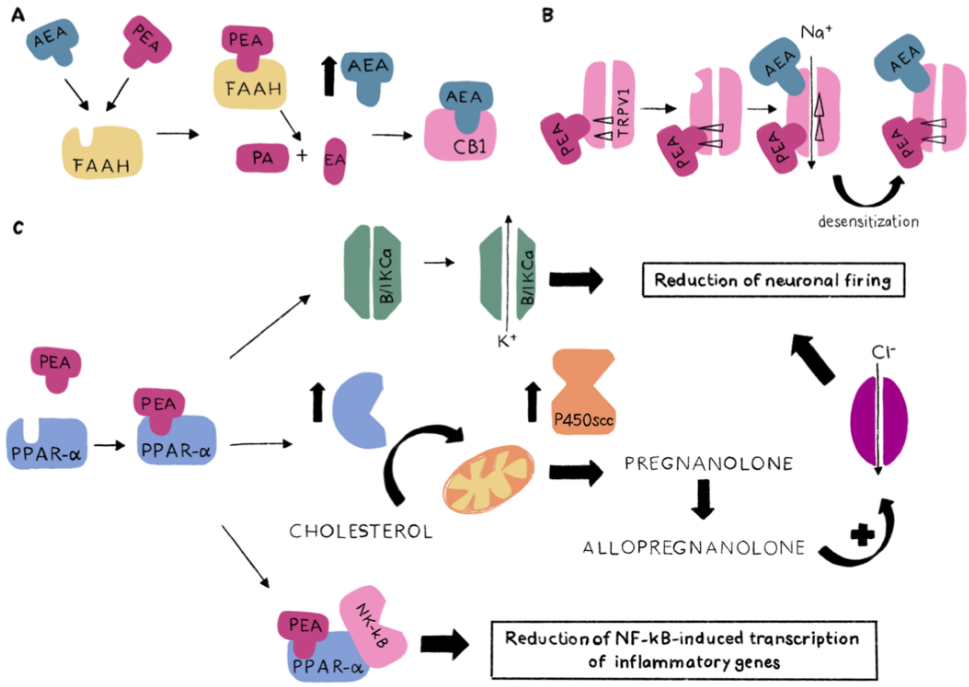

Figure 1.3.1 Direct and Indirect mechanism of action of PEA. (A) the "entourage"effect mediated by FAAH inhibition or **(B)** allosteric activity on TRPV1. **(C)** genomic and non-genomic PPAR-□-dependent mechanisms.

1.3. Pharmacological effect: from CNS to periphery, crossing PPAR-α route.

PEA was identified as a naturally occurring lipid, isolated from soybeans, egg yolk, peanut meal and other food sources (Venables et al. 2005, Gouveia-Figueira and Nording 2014) but also in mammalian cells (mast cells, macrophages, neurons, astrocytes and microglia) and thereby it is recognized as an endogenous lipid mediator (Mattace Raso et al. 2014). Several studies demonstrated the pharmacological 'Autacoid Local Injury Antagonism (ALIA) effect' exerted by PEA (Aloe et al. 1993, Mazzari et al. 1996), increasing the scientific interest in exploring the potential and numerous pharmacological effects of this molecule.

Later, D'Agostino et al (2009) demonstrated the central mechanism responsible for its anti-inflammatory properties. The authors showed that icv PEA administration prevented the nuclear translocation of Nuclear Factor (NF)-κB and the degradation of the inhibitory IκB-α, also inhibiting mitogen-activated protein kinase (MAPK) and c-Jun N-terminal Kinase (JNK) cascades, reducing inflammation in dorsal root ganglia and peripheral hyperalgesia. All these effects were lacked in mutant PPAR-α KO mice, confirming the obligatory role of the nuclear receptor in PEA-mediated analgesic and anti-inflammatory effects.

Furthermore, the central protective effects of PEA were also demonstrated in other experimental model of neuroinflammation and neurodegenerative disorders. In an animal model of Parkinson's Disease (PD) induced by 6-hydroxydopamine (6-OHDA), PEA prevented striatal inflammation, inhibiting apoptosis and ER stress markers, triggered during PD pathogenesis (Avagliano et al. 2016).

Consistently, in primary rat neuron, PEA reduced glial response in a β-amyloid (Aβ)-induced astrogliosis, in PPAR-α dependent manner (Scuderi et al. 2011, 2014).

Peripherally, PEA exhibits its protective effects in mice model of inflammatory bowel disease. In DSS-insulted mice, PEA administration ameliorated pathological features of colon inflammation, reducing neutrophil infiltration and the activation of Toll-like receptor 4 (TLR4) signaling pathway in isolated enteric glial cells (Esposito et al. 2014). All these effects were confirmed in human biopsies of patient with ulcerative colitis and explored in PPAR-α null mice, where the anti-inflammatory activities of this ALIAmide were abolished (Esposito et al. 2014).

Likewise, in a model of DNBS-induced colitis, the anti-inflammatory effects of PEA were amplified by coadministration of capsazepine, a TRPV1 antagonist, but they were abolished by CB_2, GPR55 and PPAR-α antagonist (Borrelli et al. 2015).

Moreover, the inhibitory effect on histamine, prostaglandin 2 and tumor necrosis factor (TNF) α was also reported in canine mast cell freshly isolated from skin biopsies (Cerrato et al. 2010) and in hypersensitive Beagle dogs (Cerrato et al. 2012). All these findings support the idea that, holding its anti-inflammatory properties, PEA-protective effects occur via several and correlate mechanisms, mainly mediated by PPAR-α activation and dependent by cell type and its localization.

1.4 Pharmacokinetic profile and clinical reports on PEA- based formulation.

PEA has been proposed as a valid tool in a wide range of therapeutic areas. Current clinical trials aim to investigate the role of PEA in controlling

several types of pain (i.e. lumbosciatic pain, fibromyalgia, chronic pelvic pain, neuropathic pain) (Gabrielsson et al. 2016). The authors reported a well-tolerated profile and a good efficacy of PEA-based formulations. Despite the numerous availabilities of preclinical and clinical findings, very little data are provided concerning the pharmacokinetic features of PEA. Petrosino et al (2016) reported the graphical distribution of oral micronized-PEA (2–10 μm range) administered in healthy volunteers, with a maximum plasma level at the 2h time point (from ~10 to ~23 pmol ml−1 plasma). In a more recently work, the same authors showed a comparative animal study between the non-micronized and the ultramicronized (um) PEA. The authors showed a plasma peak concentration of um-PEA after 5 min and 30 min post administration in healthy and inflamed animals, respectively (Petrosino et al. 2018).

Several reports showed the effectiveness of um-PEA in patients. In a retrospective study, Cruccu et al (2019) assessed the clinical importance of um-PEA treatment in low back pain-sciatica, also improving the disability related to neuropathy. The efficacy of um-PEA was also evaluated in patient with fibromyalgia syndrome (Schweiger et al. 2019), neuropathic pain (Andresen et al. 2016) and chronic pain in geriatric patients (Marcucci et al. 2016). All the aforementioned studies reported a significant reduction in pain perception and a quality of life improvement, with a low percentage of adverse outcome (i.e. gastrointestinal side effects, very common with other analgesic drugs).

Other new PEA-based formulation has been evaluated. A randomized clinical trial reported the efficacy of an association of PEA (300 mg) and Alpha-lipoic acid (300 mg) in the control of chronic prostatitis. After 12-

week treatment, the authors showed an improvement of pain, urinary discomfort and quality of life (Giammusso et al. 2017).

2. Obesity and related disorders

2.1. Obesity and NAFLD

One of the main risk factors associated with obesity is the development of NAFLD. It is well described that obese individuals own a rising prevalence of NAFLD, with a positive correlation between weight gain and chronic liver disease progression (Li et al. 2016, Kim et al. 2019).

NAFLD is defined as a cluster of liver abnormalities, in which steatosis could progress in nonalcoholic steatohepatitis (NASH) until more severe injuries as liver fibrosis and cancer. Despite NAFLD progression varies among individuals, depending on genetic risk factors and comorbidities, the bidirectional and detrimental association between NAFLD and obesity increases the risk of developing NASH Friedman et al. (2018). Differently from simple steatosis, NASH is a more serious process characterized by inflammation and fibrosis and related to adverse hepatic outcome (i.e cirrhosis and liver failure).

Although there is a growing impact on global health, the management of NAFLD is still an urgent therapeutic requirement. To date, lifestyle changes and weight loss represent the most effective intervention, even in preventing liver fibrosis (Vilar-Gomez et al. 2015). Ongoing clinical trials on liver-specific agents are rapidly investigating on new agents (i.e. FXF agonist, PPAR α/δ agonist or CCR2/CCR5 antagonist), although their long-term efficacy and safety are under consideration (Friedman et al. 2018). However, a multi-target and combined therapy are likely the most effective option, to strongly prevent NAFLD progression and control other comorbidities.

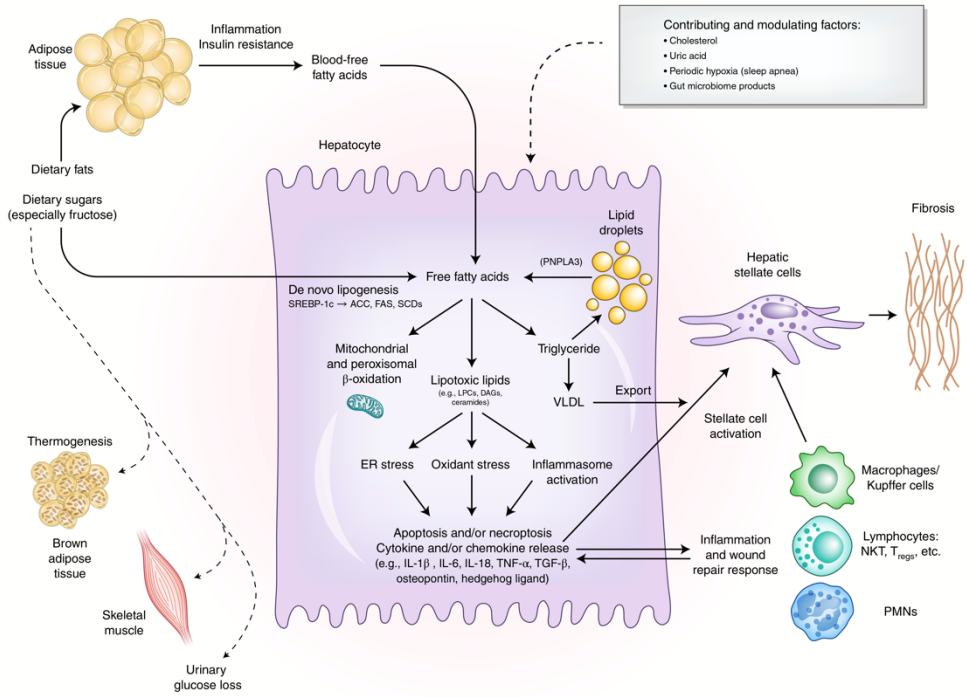

Figure 2.1.1 Pathogenic mechanism of NALFD. Circulating FFAs derived from adipose tissue lipolysis were drain to the liver. Together with hepatic de novo lipogenesis, FFAs were collected into the liver as triglycerides. When the hepatic capacity in managing lipid metabolism is overwhelmed, all these mechanisms accelerate the hepatocellular injury and inflammation, that can degenerate in stellate cell activation and progression of fibrosis (from Friedman et al, Nat Med 2018).

The pathophysiological hub linking obesity to NAFLD is the ectopic accumulation of lipids (***Fig 2.1.1***). Adipose tissue lipolysis is the primary source of free fatty acid (FFAs), a mechanism ruled by insulin signaling pathway. Overnutrition and IR leads to excessive delivery of FFAs from adipose tissue, overwhelming liver capacity in collecting nutrients. The subsequent ectopic fat accumulation results in lipo-toxicity, inducing hepatocellular injury (Friedman et al. 2018). Indeed, the toxic metabolites

trigger the activation of inflammatory pathways, driving the progression of NAFLD to NASH (Meli et al. 2014).

Noteworthy, the endocrine profile of visceral fat also affects liver homeostasis. The adipose-secreted leptin and adiponectin exert multiple regulatory functions via direct interaction with their hepatic receptor (Polyzos et al. 2015). The key role of leptin on liver function is classically represented by the development of NALFD, a paradigm occurring both in ob/ob mice, characterized by leptin deficiency, and fa/fa Zucker rats, characterized by the loss of leptin receptor (LepR) function (Pelleymounter et al. 1995, Cipriani et al. 2010). In this regard, it has been demonstrated that leptin has a bi-faceted effect. In healthy conditions, leptin prevents hepatic steatosis, but persistent hyperleptinemia worsens liver inflammation and fibrosis during NAFLD progression (Polyzos et al. 2019).

Adiponectin is the most abundant adipokine secreted by WAT. In liver, both isoform of adiponectin receptor (adipoR1 and adipoR2) are expressed (Stern et al. 2016). It has been shown that the adiponectin signaling via adipoR1 induces the activation of AMPK pathway, decreasing gene expression involved in hepatic lipogenesis and cholesterol synthesis (Awazawa et al. 2009). Moreover, the AdipoR1 activation modulates hepatic stellate cell proliferation and function (Saxena and Anania 2015). Interestingly, the adiponectin-mediated protective effect could be also related to the inhibitory interplay between leptin and adiponectin signaling (Handy et al. 2011).

Beyond the metabolic and endocrine alterations, the activation of the immune system plays a key role in the pathophysiology of NAFLD, since the liver is the main organ able to orchestrate the immune-metabolic functions (Meli et al. 2014). The detrimental activation of innate immune system induced by toxic metabolites triggers a phenomenon known as

"metaflammation" or meta-inflammation (Caputo et al. 2017). During obesity, the recruited and the resident macrophages (Kupfer cells) orchestrate the inflammatory response, which mediated the progression of simple steatosis to NASH (Meli et al. 2014). Moreover, the low-grade inflammation characterizing obesity establishes a vicious cycle between adipose tissue and liver through the releasing of pro-inflammatory cytokines (i.e. IL-6 and TNF-α) mainly involved in IR (Sabio et al. 2008, Caputo et al. 2017).

2.2. Mitochondrial dysfunction and NAFLD

Obesity and IR are both characterized by an excessive energy intake and an insufficient fat processing that lead to lipid accumulation (Mollica et al. 2017). The inability in consuming fatty acids results in inflammation, oxidative stress and mitochondrial dysfunction (Mansouri et al. 2018). Indeed, mitochondria manage the bioenergetic function of the cells, regulating i) ATP production by oxidative phosphorylation (OXPHOS), ii) the generation and detoxification of reactive oxygen species (ROS) modulating redox state and iii) ensuring cell survival (Mansouri et al. 2018). Cellular bioenergetics is partially a *futile* process, that dissipate free energy and reduce the amount of ATP generated for each molecule of oxygen that splits by the electron transport chain. The uncoupling between energy releasing and ATP production results in the *proton leak*, by which mitochondria generate an inefficient metabolism, loosing energy as heat (Bouillaud et al. 2016).

Proton leak also regulates redox state, preventing an excessive ROS production and subsequent oxidative stress, two central features of metabolic disorders (Diano and Horvath 2012) .

Moreover, AMPK is a sensor of ATP and manages energy metabolism stimulating glucose, fatty acid oxidation and peroxisome proliferator-activated receptor gamma coactivator 1-α (PGC1-α) activity (Herzig and Shaw 2018). PGC1α and PPAR-α activates the expression of crucial enzymes involved in fatty acid oxidation and mitochondrial biogenesis, ensuring metabolic homeostasis (Mansouri et al. 2018).

Since the pivotal role of mitochondria in energy metabolism, the impairment of hepatic mitochondria is a crucial driver of metabolic diseases (de Mello et al. 2017). Indeed, NAFLD patients displayed a compromised mitochondrial respiration due to IR, which leads to oxidative stress, lipid peroxidation and mitochondrial damage during the progression of liver injury (Koliaki et al. 2015). Beyond the functional perturbations, electron microscopy reveals also a morphological change in mitochondria both in preclinical model of chronic liver disease and in patient with NAFLD (Paradies et al. 2014, Mollica et al. 2017). Mitochondrial morphology is dynamic and sensitive to metabolic alterations. Depending on metabolic state, the high plasticity of these organelles results in several morphological changes, controlled by fission and fusion events (Wai and Langer 2016). Optic atrophy 1 (Opa1) protein and mitofusin (Mfn) 1 and 2 participate to mitochondrial fusion, whereas dynamin-related protein (Drp) 1 and fission protein (Fis) 1 are involved in fission (Westermann 2010).

Consistently, the balance of fission and fusion can be modulated in either direction by changes in nutrient availability and metabolic demands, leading to fragmented or hypertubular mitochondria (Wai and Langer 2016). During

a healthy status, cells maintain their mitochondria in a fragmented state, while under stress condition, such as fasting or starvation, mitochondria persist in a fused or elongated state. Interestingly, this specific stress response or hyperfusion allows mitochondria to escape the autophagic mechanism and maintain ATP levels, ensuring cell viability (Gomes and Scorrano 2011). On the other hand, a persistent fusion or an unbalanced fission induces the accumulation of giant or small and damaged mitochondria leading to an increased ROS production (Lopez-Lluch 2017).

2.3. Targeting liver in NAFLD: focus on PPAR-α

Among the well characterized drugs, several trials reported the efficacy of PPARγ ligands including thiazolidinediones (TZDs) in ameliorating steatosis, inflammation and hepatic fibrosis (Sanyal et al. 2010). However, typical side effects of TZDS (i.e. weight gain, fluid retention and osteopenia) limit their clinical use.

Recently, the farnesoid X receptor (FXR) has been candidate as a useful pharmacological target, since its activation attenuated steatosis both in rodents and humans (Tanaka et al. 2017). The hepatoprotective effect of obeticholic acid (OCA), an FXR agonist, has been investigated in several animal studies (Pellicciari et al. 2002, Mudaliar et al. 2013) and ongoing clinical trial are determining its efficacy and tolerability in human (NCT02548351). Furthermore, in an animal model of NASH, the beneficial effect of the fibroblast growth factor (FGF)19 has been addressed to its binding with FXR (Nies et al. 2015). Current clinical trials are now investigating the efficacy of some analogues of FGF19, which promote a

significant reduction of hepatic fat, without the proliferative and tumorigenic properties characterizing FGF19 activity (Harrison et al. 2018). Notably, the dual chance in targeting PPAR-α and δ or PPAR-α and γ was considered a useful therapeutic tool. Elafibrinor is the prototype of the PPAR-α/δ agonist class. Harnessing the anti-inflammatory activity of PPAR-δ and the metabolic effects of PPAR-α activation, elafibrinor has been demonstrated as a valid compound in improving metabolic features of NASH and a phase 3 clinical study is now evaluating its safety (Ratziu et al. 2016) (NCT02704403)

PPAR-α is a nuclear receptor mainly expressed in liver, heart and brown adipose tissue, involved in inflammation and metabolic control, especially during fasting (Bougarne et al. 2018). The key role of PPAR-α in lipid metabolism is clearly described in liver specific PPAR-α null mice, which displayed an impairment of hepatic lipid homeostasis in aging (Montagner et al. 2016). The activation of hepatic PPAR-α is mediated by extra- and intra-cellular signals and depend on nutrient status, establishing a mutual and perpetuated communication among metabolic organs (i.e adipose tissue, pancreas, liver and blood stream) (***Fig. 2.3.1***) (Pawlak et al. 2015).

During fasted state, PPAR-α triggers FAO and ketogenesis, directly inducing β-oxidation and enhancing FGF21 plasma levels (Inagaki et al. 2007). Moreover, the sensor AMPK stimulates the energy production, activating PPAR-α-target genes. Based on central role of this receptor in metabolism, PPAR-α is considered a harmful target in controlling lipid homeostasis. Actually, fibrates are PPAR-α agonist approved for dyslipidemia, also preventing cardiovascular and coronary events, but with low safety profile (Tanaka et al. 2017).

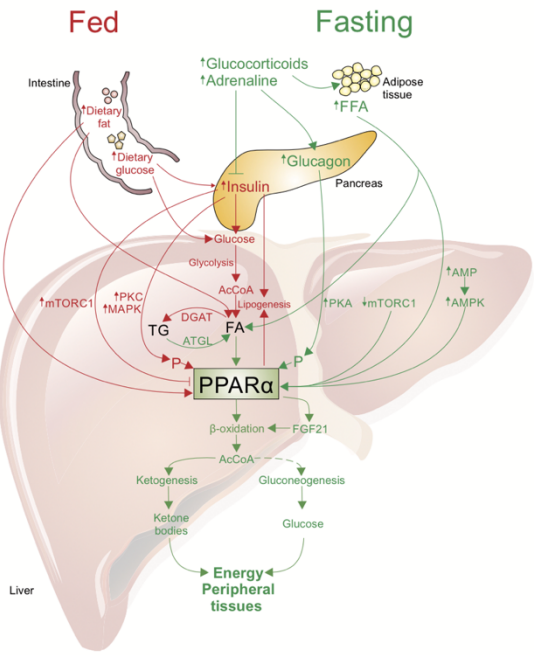

Figure 2.3.1 Molecular regulation of PPAR-α activity during fasted or fed state. After feeding, insulin enhances PPARα phosphorylation and its transcriptional activity. Moreover, also lipogenesis yields fatty acid -derivatives which act as PPARα ligands. In the fasted state, glucagon triggers PKA-dependent PPARα activity. Adipose tissue lipolysis raises plasma levels of FFAs, subsequently collected in the liver as triglycerides. The hydrolysis of hepatic intracellular triglycerides produces lipid ligands for PPARα. Furthermore, prolonged fasting increases the amount of AMP, inducing AMPK to stimulate energy production driving fatty acid oxidation via PPARα. Its activation increased FFAs oxidation, gluconeogenesis, ketone body synthesis and thus maintain energy source for peripheral tissues (from Pawlak et al, J Hepatol 2015)

2.4. Obesity and adipose tissue dysfunction

The worldwide prevalence of obesity increased the scientific interest in the study of adipose tissue. Until 1940s, adipose tissue was commonly recognized as an inert tissue able to store lipids. Only 50 years later, the discovery of leptin changed the common perception, and promoted the onset of several pioneering investigation on this tissue as adipose organ and, its role in health and disease (Rosen and Spiegelman 2014).

Adipose tissue can be defined as a multi-depot organ with a peculiar anatomy, vascularization, innervation and cytology (Cinti 2012). The key function of fat is the regulation of energy balance and nutrient homeostasis, that are critically compromised during obesity.

The main feature of adipose organ consists in the ability to change its dimensions, not only by expanding the size of a single cell (hypertrophy), but also increasing the number of resident cell (hyperplasia) (Rosen and Spiegelman 2014). More recently, it has been demonstrated that in human total cell number was established during childhood and maintained in the life span (Spalding et al. 2008). Indeed, weight loss is mainly due to a significant reduction in adipocyte volume and only few differences are detectable in the overall number of cells, indicating that the adiposity should be finely tuned during childhood (Spalding et al. 2008).

Upon overnutrition, the dramatic changes occurring in the adipocytes reach a threshold, beyond which their ability in size expansion becomes limited; this phenomenon triggers stress-related events, including hypoxia, inflammation, fibrosis that contribute to cell death (Sun et al. 2013). All these phenomena modify the immune-endocrine profile of fat, sustaining the pathogenesis of obesity-related disease such as IR. Indeed, the adipose

organ secrets various bioactive factors, including adipokines involved in glucose and lipid metabolism, feeding behavior and inflammation (Kusminski et al. 2016). Among these, leptin mediates a complex multi-organ crosstalk between periphery and central nervous system. In lean, leptin reduces body weight and food intake, enhances energy expenditure via hypothalamic regulation. Leptin carries out its effect not only through the autocrine regulation but also via peripheral nervous system, as recently demonstrated by Zeng et al. (2015). Indeed, these authors elegantly showed that leptin-mediated lipolysis depends on the intact sympathetic neuro-adipose connections. On the other side, the adipokine adiponectin provides the "healthy" expansion of adipose tissue, preventing the dangerous ectopic accumulation of lipids (Stern et al. 2016). Adiponectin is also centrally involved in the control of energy homeostasis; in fact, the peripheral insulin-sensitizer effect of adiponectin promotes central leptin and insulin-mediated effects (Qi et al. 2004).

The regulation of metabolism is retained by a complex balance among energy status, adipokine secretion and neuronal control, which is deeply compromised during obesity. Recently, it has been proposed a triangular relationship among adipocytes, immune cell and sympathetic nervous system, highlighting the complex features of obesity (***Fig 2.4.1.***) (Larabee et al. 2020). Under chronic inflammation the adipose tissue resident macrophages (ATM's) could regulate sympathetic innervation by degrading noradrenaline, and thus reducing its bioavailability (Camell et al. 2017).

In light of these considerations, a pleiotropic molecule operating at multiple level of metabolic control may offer a practicable therapeutic approach to limit obesity and the related decline of metabolic function.

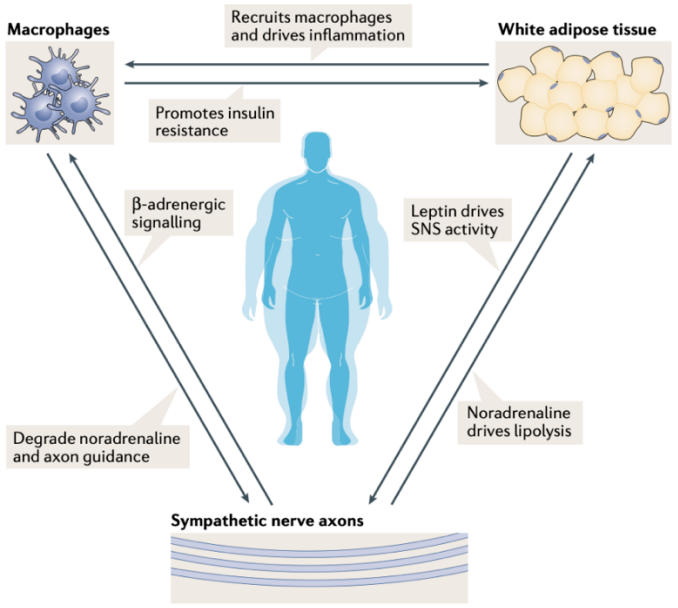

Figure 2.4.1 The neuroimmunoendocrine triangle. In obesity, macrophages- derived cytokines provoke insulin resistance in adipose tissue and drive chronic systemic inflammation. Sympathetic nervous cues promote lipolysis, browning and thermogenesis, sustaining energy metabolism. Under chronic inflammatory status, not only endocrine factor, but also macrophages could dampen SNS-adipose tissue relationship, contributing to the onset of obesity (from Larabee et al 2020, Nat Rev Endrocinol)

2.5. The "shadow" of fat

Adipose organ composition varies in its cytology, depending on distinct role and anatomic localization (Cinti 2002). Two types of adipocyte can be distinguished: unilocular **white adipocytes**, whose cytoplasmic volume is due to a large lipid droplet, and **brown adipocytes**, polygonal cells composed by several lipid droplets and numerous mitochondria packed with cristae (Cinti 2002). Unilocular adipocytes appeared white and therefore are the main cellular phenotype composing white adipose tissue (WAT) (***Fig. 2.5.1***). On the contrary, the numerous mitochondria give a brown appearing

to the multilocular adipocytes and justifying the name of brown adipose tissue (BAT) (***Fig. 2.5.1***). The morphological differences between white and brown adipocytes mirror their distinct role in physiology. Indeed, white adipocytes store lipid as nutrient source, whereas brown adipocytes are highly specialized cells that burn energy to produce heat (thermogenesis) (Giordano et al. 2016).

BAT provides non-shivering thermogenesis via uncoupling protein (UCP)1. UCP1 is a BAT-specific protein and catalyzes the proton leak across the inner mitochondrial membrane, by which fuel oxidation results in an "uncoupled" process from ATP synthesis (Nedergaard et al. 1977, Chouchani et al. 2019). BAT activation requires environmental stimuli: cold exposure, diet and noradrenergic signals trigger heat production (Giordano et al. 2016). Indeed, BAT is highly innervated, and the balanced and intact noradrenergic nerve tone is obligatory to maintain tissue physiology (Fischer et al. 2019).

Nowadays, adipose tissue is recognized as convertible and plastic organ, able to transdifferentiate (***Fig. 2.5.2***) (Giordano et al. 2016). The adipocyte reprogramming depends on body's energy status; cold exposure, exercise and adrenergic stimuli lead to thermogenic requirement and thus white-to-brown transdifferentiation, whereas overnutrition enhance brown-to-white phenotype and allow energy storage (Giordano et al. 2016). Indeed, in obese animal WAT increases at the expense of BAT, a phenomenon known as "whitening". On the contrary, "browning" consists in an increase of BAT and in the appearance of UCP1-positive cell in white fat depots (***Fig. 2.5.1***) (i.e in subcutaneous or inguinal fat pad) (Loncar 1991). These brown-like cells are known as beige/brite (*br*own and wh*ite*) adipocyte (Harms and Seale 2013). The mechanisms underpinning the browning has been deeply

investigated: lineage tracing approach demonstrated that inducible beige cells could be derived either from white adipocyte transdifferentiation or resident brown precursor proliferation and differentiation (Wang et al. 2013).

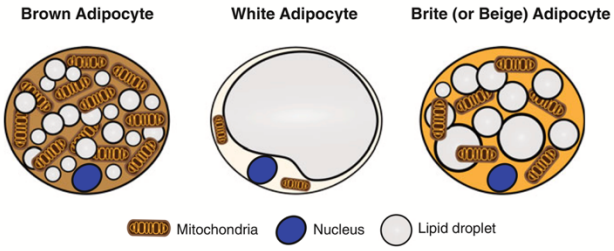

	Brown	*White*	*Brite/beige*
UCP1 Expression	Positive	Negative	Positive
Mitochondrial Density	High	Low	Medium
LD Morphology	Multi-locular	Uni-locular	Multi-locular
Primary Function	Thermogenesis Endocrine	Energy storage Endocrine	Thermogenesis? Endocrine?

Figure 2.5.1. Brown, white and beige adipocytes features (from Handbook of experimental pharmacology, Pfeifer et al 2019).

Cell lineage-tracing studies allowed to define the developmental origin of brown and white adipocytes. Adipocytes develop from pre-adipocytes, which origin from stromal vascular fraction (endothelial cell or pericytes) (Cinti 2018). At the transcriptional level, the master regulator of adipogenesis is PPAR-γ, that is necessary to drive adipocyte formation (Rosen and Spiegelman 2014).

The scientific community had previously assumed that brown and white adipocytes shared the same developmental genetic pattern. Later findings

clarified that, differently from unilocular congener, brown adipocytes develop from a common cell precursor of skeletal muscle.

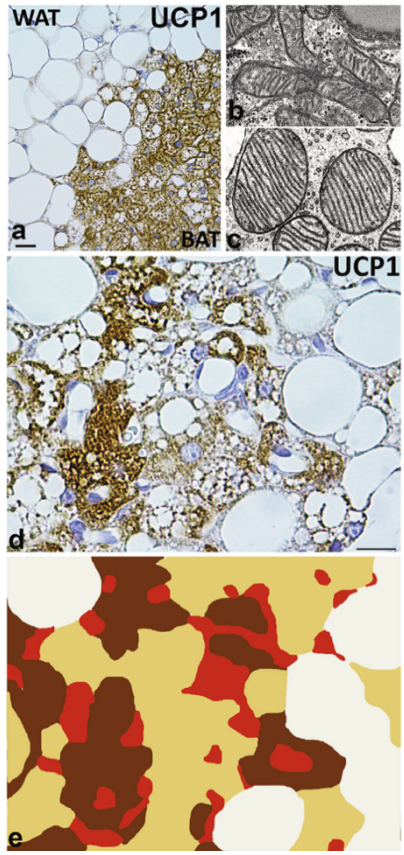

Figure 2.5.2. Light microscopy and Transission Electron Microscopy of white and brown adipose tissue of interscapular area of C57BL/6J cold exposed mouse. The panel ***a*** shows WAT, on the right, mainly composed by unilocular adipocytes, and on the left BAT. Bar: 10 μm. In ***b*** mitochondria of WAT with randomly oriented cristae, and in ***c*** mitochondria of BAT, highly organized in laminar cristae. Bar: 0.5 μm. ***d***, mixed area composed by adipocytes with different morphology, immunostained for UCP1. Multilocular cells are more immunoreactive compared to paucilocular (weakly immunostained-beige) and unilocular cells (not immunostained). ***e,*** representative scheme clustering the three type of cell (brown, white and beige; red: capillaries) (from Cinti S, Curr Opinion Endocrine and Metabolic Research 2019).

The transcriptional regulation is orchestrated by homologous domain-containing protein-16 (PRDM16), which drives the switch from myoblasts to brown fat (Seale et al. 2007).

Interestingly, PGC1α provides further transcriptional regulation of mitochondrial biogenesis, oxidative metabolism and thermogenesis of brown fat and PGC1α genetic ablation impaired the expression of some thermogenic markers (Puigserver and Spiegelman 2003).

The pharmacological research aims to discover target and molecules to switch on beige phenotype and to harness adipose organ plasticity which may provide a novel approach to limit obesity and related disorders.

2.6. Targeting adipose tissue: a novel potential therapeutic tool.

In the last few decades, the mechanism involved in energy homeostasis and browning phenomenon have been explored.

In table 1, are reported the current drugs approved for the pharmacotherapy of obesity. Among these, liraglutide has the most important clinical significance. Liraglutide is an analog of glucagon-like peptide (GLP) 1, approved in 2010 by US Food and Drug Administration. Clinical evidence suggests that liraglutide not only ameliorates insulin-sensitivity but also induce a significant weight loss (Astrup et al. 2009). Interestingly, the weight-reducing effect of liraglutide in humans was associated to the BAT activation and to the increased energy expenditure induced by the hypothalamic AMPK signaling pathway (Beiroa et al. 2014). Indeed, energy homeostasis is regulated by several and integrated mechanisms that represent many pharmacological targets able to counteract overweight. Beyond the regulation of central feeding behavior, the possibility to

peripherally induce WAT browning and BAT activation have been considered as a potential anti-obesity therapeutic tool.

Drug	Mechanism of Action
Phentermine (Adipex-P®)	NE transporter inhibitor; Appetite suppression mediated by activation of POMC neurons in the arcuate nucleus
Orlistat (Xenical®)	Gastric- and pancreatic-lipase inhibitor; Reduces absorption of dietary fat
Lorcaserin (Belviq®)	Selective 5-HT_{2C} agonist; Promotes satiety
Phentermine and Topiramate (Qsymia®)	Phentermine: NE transporter inhibitor; Appetite suppression mediated by activation of POMC neurons in the arcuate nucleus Topiramate: GABA agonist; Appetite suppression may be due to modulation of voltage-gated ion channels, increased activity at GABA-A receptors and/or inhibition of AMPA/kainite glutamate receptors
Naltrexone and Bupropion (Contrave®)	Naltrexone: Opioid receptor antagonist; Prevents β-endorphin-mediated negative feedback on α-MSH release Bupropion: DA and NE transporter inhibitor; Stimulates hypothalamic POMC neurons that release α-MSH resulting in decreased food intake and increased energy expenditure
Liraglutide (Saxenda®)	GLP-1 agonist; Decreases appetite

Table 1. FDA-approved drug to treat obesity.

In this regard, β_3 receptor agonist induced white-to-brown transdifferentiation in both subcutaneous and visceral WAT depots (Ghorbani et al. 1997). Mirabegron is a latest generation β_3 -adrenoreceptor agonist, with a more specific pharmacodynamic profile (Takasu et al. 2007) and able to increase energy expenditure via BAT activation (Cypess et al. 2009). To date, mirabegron is widely prescribed in urological disease, and recently several findings are emerging on its safety and therapeutic potential in obesity (Hao et al. 2019, Loh et al. 2019). Unfortunately, β -

adrenoreceptors are not a specific target of browning, and the adverse cardiovascular outcomes could occur (Arch 2011).

Sirtuin 1 (SIRT1) is a histone deacetylase type III, belonging to the family of Sirtuin. SIRT1 is an NAD^+-dependent deacetylase involved in metabolic regulation and adaptation to caloric restriction (Chang and Guarente 2014). Among its effect, SIRT1 induces brown remodeling in scWAT via PGC1α (Qiang et al. 2012). The natural polyphenol resveratrol has been identified as a SIRT1 allosteric activator, able to activate oxidative metabolism in BAT and ameliorate IR (de Ligt et al. 2015).

Moreover, the altered balance of adipose tissue homeostasis depends on a pro-inflammatory status, that makes the inflammatory pathways an attractive therapeutic target for the treatment of obesity. Indeed, adipocyte hypoxia, mechanical stress, and cell death contribute to peripheric IR and ineffective hormone responsiveness, sustaining the etiopathogenesis of obesity and metabolic disorders (Reilly and Saltiel 2017). Indeed, some clinical trial have demonstrated that antibodies neutralizing TNF or IL-1β antagonists were effective in improving glucose metabolism in T2D patients but failed to be harmful in dampening adipose tissue inflammation (Moller 2000, Sloan-Lancaster et al. 2013). A putative problem related to the ineffectiveness of anti-inflammatory drugs in obesity is that to target a specific cytokine may not be sufficient to handle the complex inflammatory pathways involved in several processes of metabolic diseases which include different inflammatory cytokines, mediators and enzymes (Reilly and Saltiel 2017).

3.Materials and Methods

3.1. In vivo procedures

3.1.1. Mouse model of HFD-induced obesity

Male C57Bl/6J mice (Harlan, Italy) at 6 weeks of ages, were housed in stainless steel cages in a room kept at 22±1°C with a 12:12 hours light-dark cycle. Standard chow diet (Mucedola srl, Milan, Italy) had 17% fat, without sucrose while HFD (Research Diets Inc, NJ, USA) had 45% of energy derived from fat, 7% of sucrose. Standard and HFD contained 15,8 and 21,9 kJ/g, respectively, determined by bomb calorimeter. Moreover, the diet composition formula, the detailed fatty acid profile and the relative percentage of monounsaturated and saturated fatty acid of STD diet and HFD are reported in ***Table 2 and 3***.

	STD	**HFD**
Diet composition	**%**	**%**
Protein	29	21,2
Carbohydrate	60,4	24
Fat	10,6	54,8
Energy, kJ/g	15,88	21,9

Table 2. Diets composition formula

Fatty acid profile	STD	HFD
	%/total fat	%/total fat
C10, Capric	-	0,056
C12, Lauric	0,232	0,085
C14, Myristic	1,16	1,101
C15	-	0,073
C16, Palmitic	14,83	19,29
C16:1, Palmitoleic	0,929	1,311
C17	-	0,353
C18, Stearic	3,252	10,38
C18:1, Oleic	19,783	33,61
C18:2, Linoleic	50,25	29,47
C18:3, Linolenic	9,562	2,202
C20, Arachidic	-	0,209
C20:1	-	0,608
C20:2	-	0,734
C20:3, n6	-	0,105
C20:4, Arachidonic	-	0,262
C22, Behenic	-	0,052
C22:5, Docosapentaenoic	-	0,080

Table 3. Relative percentage of monounsaturated and saturated fatty acid of STD diet and HFD

After weaning, young mice were randomly divided into three groups as follows: control group (STD) receiving chow diet and vehicle *per os* by gavage; 2) HFD group receiving vehicle; 3) HFD group treated with PEA (HFD+PEA, 30 mg/kg/die *per os*, by gavage). The treatments started after

12 weeks of HFD feeding and lasted 8 weeks (***Fig.3.1.1.***). Ultra-micronized PEA was provided by Epitech Group Research Labs (Padova, Italy). It was suspended in carboxymethyl cellulose (1,5%) for oral gavage.

The animals were anaesthetized by enflurane followed by cervical dislocation and serum and tissues (liver, BAT and iWAT) were collected. Liver from all mice was removed and the samples not immediately used for mitochondria preparation were frozen and stored at -80°C for subsequent biochemical determinations.

3.1.2. Validation of in vivo experimental model.

During the experimental period, body weight was weekly assessed. At the end of experimental protocol (***Fig. 3.1.2.1.***), before sacrifice, bioelectrical impedance analysis was performed to determine fat body composition assessment using BIA 101 analyzer, modified for the mouse (Akern, Florence, Italy).

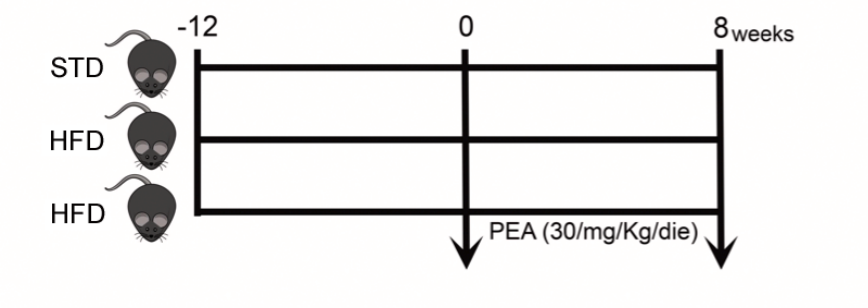

Figure 3.1.1. *In vivo* experimental design

3.1.3. Energy intake measurement

The total energy intake was calculated considering the weekly food intake and the energy content of the diets.

Energy intake (EI) was obtained using the following equation:

EI = food intake × energy food intake (Moir et al. 2016).

Food intake of group housed mice was weekly measured. Energy intake was calculated considering the gross energy content of the diets, 15,8 and 21,9 kJ/g for chow diet and HFD respectively, both values determined by bomb calorimeter.

3.1.4. Measurement of oxygen consumption (VO2), carbon dioxide production (VCO2) and respiratory quotient (RQ)

Upon an adaption period to the experimental environment (at least 1 day) in the metabolic-monitoring apparatus, VO2 and VCO2, were recorded by a monitoring system (Panlabs.r.l., Cornella, Barcelona, Spain) composed of a four-chambered indirect open-circuit calorimeter, designed for continuous and simultaneous monitoring. VO2 and VCO2 were measured every 15 min (for 3 min) in each chamber for a total of 6 hours (from 8:00 am to 14:00 pm). The mean VO2, VCO2 and RQ values were calculated by the "Metabolism H" software (Dominguez et al 2009). (Dominguez et al. 2009)

3.2. Morphological studies

3.2.1. Animal procedures

A subset of animals was euthanized with an overdose of anesthetic (Avertin; Fluka Chemie, Buchs, Switzerland) and immediately perfused with 4% paraformaldehyde in 0.1 M phosphate buffer (PB), pH 7.4. Liver, BAT and

subcutaneous WAT (sWAT) depots were dissected and further fixed by immersion in 4% paraformaldehyde in PB overnight at 4 °C. Thus, the tissues were dehydrated in ethanol, cleared in xylene, and embedded in paraffin.

3.2.2. Hepatic histological analysis

Paraffin-embedded 4 μm liver sections were stained with hematoxylin and eosin (H&E) for morphology. Unfixed cryostat 10 μm liver sections were stained with Oil Red O (# 04-220923, Bio Optica, Milan, Italy) according to manufacturer's instruction to measure intracellular lipid droplet accumulation. A double-blinded examination of the sections was made at a magnification x200 with a concordance rate of 95%.

For histological score analysis, three main broad categories of histological features were analyzed: steatosis, inflammation and necrosis. The grading system was adapted from Kleiner et al. as previously described (Kleiner et al. 2005, Oriente et al. 2013). Kleiner's grading system considers the following histological variables:

i) severity of steatosis (quantified by low- to medium-power evaluation of parenchymal involvement by steatosis): score 0, <5%; score 1, 5–33%; score 2, >33–66%, score 3, >66%; ii)

ii) location (predominant distribution pattern): zone 3, score 0; zone 1, score 1; azonal, score 2;

iii) inflammation: lobular inflammation (overall assessment of all inflammatory foci): score 0, no foci; score 1, <2 foci per ×200 magnification field; score 2, 2–4 foci per ×200 magnification

field; score 3, >4 foci per ×200 magnification field; necrosis: score 0, present; score 1, absent.

Statistical analysis was performed using SPSS software (P<0,05). The comparison among groups was performed using ANOVA univariate analysis.

3.2.3. Light microscopy and morphometry on adipose tissue depots

Serial paraffin sections (3μm thick) were obtained from each adipose depot, placed on glass slides, and dried. Alternate sections were stained with H&E to assess morphology, and for immunohistochemical procedures to evaluate tissue protein expression. Tissue sections were examined with a Nikon Eclipse E800 light microscope, and digital images were captured at 10X and 20X with a Nikon DXM 1200 camera (Nikon Instruments S.p.A, Calenzano, Italy). Adipocyte areas was measured with the open-source image analysis software ImageJ v1.46r (Rasband, WS, ImageJ; National Institutes of Health). For each group, 5 fields from each of 5 different H&E-stained section per animal were analyzed.

For immunohistochemistry, 3-μm-thick paraffin-embedded sections of the fat depots were dewaxed, treated with 10% H2O2 for 5 min to block endogenous peroxidase, rinsed with PBS, and incubated in 3% normal serum blocking solution (in PBS; 30 min). BAT sections were then incubated overnight at 4 °C with sheep polyclonal anti Tyrosine Hydroxylase (TH) antibody (Merk-Millipore, Massachusetts, United States), rabbit polyclonal UCP1, (diluition 1:1000, Abcam, Cambridge, UK) a tissue specific mitochondrial protein and SC section were stained with rat monoclonal anti-MAC-2 antibody (dilution 1:3000; Cedarlane

Laboratories, Burlington, Ontario, Canada), a marker of activated macrophages. After a thorough rinse in PBS, sections were incubated in 1:200 v/v, rabbit anti-sheep (TH schedule) or goat anti-rabbit (UCP1 schedule), horse anti-mouse (MAC-2 schedule) IgG biotinylated HRP-conjugated secondary antibody solution (Vector Laboratories, Burlingame, CA, USA) in PBS for 30 min. Histochemical reactions were performed using Vectastain ABC Kit (Vector Laboratories) and Sigma Fast 3,3′-diaminobenzidine (Sigma-Aldrich, Vienna, Austria) as substrate. Sections were counterstained with hematoxylin, dehydrated in ethanol, and mounted in Eukitt® Mounting Medium (Sigma-Aldrich). Staining was never observed when the primary antibody was omitted.

TH density was determined randomly dividing the sections (n=7) in 6 field and counting the total number of positive fibers in each section compared to the total number of adipocytes and was expressed as TH fibers number/100 adipocytes.

3.3. Biochemical analysis

3.3.1. Serum and hepatic parameters and tissue isolation

At the end of the experimental period (8th week), the sera and livers were collected. In serum, alanine aminotransferase (ALT), aspartate aminotransferase (AST), triglycerides and total cholesterol were measured by colorimetric enzymatic method using commercial kits (SGM Italia, Italy and Randox Laboratories ltd., United Kingdom). Serum interleukin (IL)-1, IL-10, (Thermo Scientific, Rockford, IL, USA), tumor necrosis factor- α (TNF-α), and monocyte chemoattractant protein-1 (MCP-1) (Biovendor R&D, Brno, Czech Republic), adiponectin and leptin (B-Bridge International Mountain View, CA) concentrations were measured using commercially available ELISA kits. Liver samples were homogenized in saline solution and then centrifuged at 5000 rpm for 5 minutes. Supernatants were collected and centrifugated at 14.000 rpm at 4 ˚C for 15 minutes and triglycerides quantified (TGL Flex reagent cartridge, Siemens Healthcare GmbH, Erlangen, Germany).

3.3.2. Western blotting

Tissues (liver and sWAT) were homogenized and cells lysed, and total protein lysates were undergone to SDS-PAGE. The filter was probed with a rabbit polyclonal antibody against anti-phospho AMPK or anti-AMPK, (dil 1:1000, Cell Signaling Technology, Danvers, MA, USA), anti-PPAR-α (dil. 1:500 Sigma-Aldrich, Milan, Italy), anti-PPARGC1α (dil. 1:1000, PGC1α, Elabscience, Houston, Texas), and anti-CPT1, anti-mitofusin (MFN)2, -

dynamin-related protein (DRP)1 and -fission protein (Fis)1 (dil. 1:1000, Santa Cruz Biotechnology, Inc., Santa Cruz, CA), or anti-suppressor of cytokine signaling 3 (SOCS3) (dil. 1:1000, Santa Cruz Bio- technology, Inc), or phosphorylated signal transducer and activator of transcription 3 (pSTAT3) or STAT3 (dil 1:1000, Cell Signaling Technology).

Western blot for Tubulin and β-Actin (dil. 1:5000, Sigma-Aldrich, Milan, Italy) were performed to ensure equal sample loading. Bands were detected by ChemiDoc imaging instrument (Bio-Rad, Segrate, Italy).

3.3.3. Real-Time semi-quantitative PCR

After treatment, total RNA of liver and HepG2 cells was extracted using TRIzol Reagent (Bio-Rad Laboratories) and following a specific RNA extraction kit (NucleoSpin®, MACHEREY-NAGEL GmbH & Co, Düren, Germany), according to the manufacturer's instructions. Total RNA of adipose tissue (BAT and iWAT) was obtained using RNeasy Lipid Tissue (Qiagen, Hilden, Germany). cDna was synthesized using High-Capacity cDNA Reverse Transcription Kit (Applied Biosystems). PCRs were performed with a Bio-Rad CFX96 Connect Real-time PCR System instrument and software (Bio-Rad Laboratories). Each cDNA sample (500 ng) was mixed with 2X QuantiTech SYBRGreen PCR Master Mix and validated primers *Ppara*, *Fasn, Tnfa, Il6*, *Ucp1, Ucp2, Prdm16, Ppargc1a, Fabp4*, *Il10, Pparg, AdipoQ* (Qiagen, Hilden, Germany). The relative amount of each studied mRNA was normalized to *Actb* for liver and iBAT and *Rn18s* for scWAT as a housekeeping gene, and the data were analyzed according to the $2^{-\Delta\Delta Ct}$ method. Real-Time PCR was performed by CFX96 instrument (Bio-Rad, Segrate, Italy).

3.3.4. Mitochondrial oxidative capacity and degree of coupling

In another set of animals, the mitochondrial isolation, oxygen consumption, and the degree of coupling measurements were performed as previously reported (Lama et al. 2017).

Briefly, the livers were freshly collected and washed in a medium containing 220 Mm mannitol, 70 mM sucrose, 20 mM N2-(hydroxyethyl) piperazine-N-2-ethanesulfonic acid (HEPES) (pH 7.4), 1 mM-EDTA, and 0.1 % w/v fatty acid free BSA. Tissue fragments were homogenized with the above medium (1:4, w/v) in a Potter Elvehjem homogenizer (Heidolph, Kelheim,Germany) set at 500 rpm (4 strokes/min). The homogenate was centrifuged at 1000 gav for 10 min and the resulting supernatant fraction was again centrifuged at 3000× g for 10 min. The mitochondrial pellet was washed twice and finally resuspended in a medium containing 80mMKCl, 50 mM HEPES (pH 7.0), 5 mM KH_2PO_4, and 0.1% w/v fatty acid free BSA. The protein content of the mitochondrial suspension was determined by the method of Hartree using BSA as the protein standard (Hartree 1972). Isolated mitochondria were then used for the determination of respiratory parameters.

Oxygen consumption was measured in the presence of substrates and ADP (state 3), in the presence of substrates alone (state 4) and their ratio (respiratory control ratio, RCR) were calculated. The substrates used for liver respiration were 10 mM succinate + 3.75 µM rotenone or 40 µM palmitoylcarnitine + 2.5mM malate for the determination of FAO rate.

The degree of coupling was determined in the liver by applying equation by Cairns et al. (1998) of coupling = $\sqrt{1 - (Jo)_{sh}/(Jo)_{unc}}$ where $(Jo)_{sh}$

represents the oxygen consumption rate in the presence of oligomycin that inhibits ATP synthase, and $(Jo)_{unc}$ is the uncoupled rate of oxygen consumption induced by carbonyl cyanide trifluoromethoxyphenylhydrazone (FCCP), which dissipates the transmitochondrial proton gradient. $(Jo)_{sh}$ and $(Jo)_{unc}$ were measured as above using succinate (10 mmol/L) rotenone (3.75 μmol/L) in the presence of oligomycin (2 μg/mL) or FCCP (1 μmol/L), respectively. Aconitase activity was measured spectrophotometrically (at 412 nm). Determination of aconitase specific activity was carried out in a medium containing 30mMsodium citrate, 0.6mMMnCl2, 0.2 mM NADP, 50 mM TRIS-HCl pH 7.4, and two units of isocitrate dehydrogenase. The formation of NADPH was followed spectrophotometrically (340 nm) at 25°C (Alexson and Nedergaard 1988). The level of aconitase activity measured equals active aconitase (basal level). Aconitase inhibited by ROS in vivo was reactivated so that total activity could be measured by incubating mitochondrial extracts in a medium containing 50 mM dithiothreitol, 0.2mM Na_2S, and 0.2mM ferrous ammonium sulphate (Hausladen and Fridovich 1996).

Carnitine-palmitoyl-transferase (CPT) activity was determined spectrophotometrically as CoA-sH production by the use of 5,5'-dithiobis (nitrobenzoic acid) (DTNB) and palmitoyl-CoA 10 μM, as substrate. The medium consisted of 50 mM KCl, 10 mM Hepes (pH 7.4), 0.025% Triton X-100, 0.3 mM DTNB, and 10–100 pg of mitochondrial protein in a final volume of 1.0 ml. The reaction was followed at 412 nm with spectrophotometer, and enzyme activity was calculated from an E412 = 13,600/ (M X cm). The temperature was maintained at 25°C. Aconitase activity was measured spectrophotometrically (412 nm). Determination of aconitase specific activity was carried out in a medium containing 30mM

sodium citrate, 0.6mM $MnCl_2$,0.2 mM NADP, 50 mM TRIS-HCl pH 7.4, and two units of isocitrate dehydrogenase. The formation of NADPH was determined spectrophotometrically (340 nm) at 25°C. The level of aconitase activity measured equals active aconitase (basal level). Superoxide dismutase (SOD)-specific activity was carried out according to Flohe and Otting (1984).

3.4.5. Oxidative stress

The levels of reactive oxygen species (ROS) were also determined in liver homogenate as previously reported (Lama et al. 2017). An appropriate volume of freshly prepared liver homogenate was diluted in 100 mM potassium phosphate buffer (pH 7.4) and incubated with a final concentration of 5 μM dichlorofluorescein diacetate (Sigma–Aldrich) in dimethyl sulfoxide for 15 min at 37 °C. The dye-loaded samples were centrifuged at 12,500 × g per 10 min at 4 °C. The pellet was vortex mixed at ice-cold temperatures in 5 ml of 100 mM potassium phosphate buffer (pH 7.4) and again incubated for 60 min at 37 °C. The fluorescence measurements were performed with a HTS-7000 Plus-plate-reader spectrofluorometer (Perkin Elmer, Wellesley, Massachusetts, USA) at 488 nm for excitation and 525 nm for emission wavelengths. ROS were quantified from the dichlorofluorescein standard curve in dimethyl sulfoxide (0–1 mM).

The specific activity of aconitase and superoxide dismutase (SOD) was spectrophotometrically measured (Flohe and Otting 1984, Cavaliere et al. 2016). Catalase activity was determined based on the decomposition of H_2O_2 at 25 °C (Aebi 1984). Reduced glutathione (GSH) and oxidized

glutathione (GSSG) concentrations in the liver were measured with the dithionitrobenzoic acid-GSSG reductase recycling assay (Bergamo et al. 2007)

3.4.6. Analysis of fatty acid profiles in liver.

Extraction, purification and quantification of palmitic, palmitoleic, oleic acid and PEA from liver require several biochemical reactions. First, tissues (n=5) were homogenized and extracted with chloroform/methanol/Tris-HCl 50 mM pH 7.5 (2:1:1, v/v) containing internal deuterated standards for the analyte quantification by isotope dilution (Cayman Chemicals, MI, USA). The lipid-containing organic phase was dried down, weighed and pre-purified by open bed chromatography on silica gel. Fractions were obtained by eluting the column with 99:1, 90:10 and 50:50 (v/v) chloroform/methanol. The 90:10 fraction was used for the quantification by liquid chromatography-atmospheric pressure chemical ionization-mass spectrometry (LC-APCI-MS), as previously described and using selected ion monitoring at M+1 values for the four compounds and their deuterated homologues, as previously described (Di Marzo et al. 2001, Piscitelli et al. 2011).

3.5. In vitro studies

3.5.1. In vitro model of Insulin-Resistance (IR)

Human HepG2 cells (American Type Culture Collection, Manassas, VA) were cultured in complete RPMI 1640 medium at 37 °C with 5% CO_2. After 16 h starvation in 5% FBS medium, HepG2 cells were incubated with

sodium palmitate (Pal, 100 μM, Sigma-Aldrich, Milan, Italy) or its vehicle, for 24 h to obtain Pal-induced insulin resistant and control cells, respectively (Cao et al. 2012, Wu et al. 2014). 2 h before Pal challenge, cells were pre-treated with PEA (1 μM). Compound C (2 μM) was used as inhibitor of AMPK (Sigma-Aldrich, Milan, Italy), was added 1h before PEA stimulation. After 24 h Pal challenge, cell lipid content was evaluated or Western blot analysis on cell lysate was performed.

3.5.2. Lipid content measurement

HepG2 cells were plated into 6-well plates (5×10^4cells/well). After induction of insulin resistance with Pal 0.5mM and INS 100 nm, relative lipid content was measured. Briefly, cell monolayers were rinsed twice with 1 × PBS and fixed in 10% (vol/vol) formaldehyde in 1 × PBS for 60 min at room temperature. After washing with distilled water 2 times, fixed cells were stained with 1 mL/well of Oil Red O (ORO) working solution for 2 h. This solution was prepared as follows: 0.5 g of ORO was dissolved in 100 mL of absolute isopropanol and kept overnight, then filtered through Whatman no. 1 filter paper. The filtrate was diluted with distilled water (6:4 vol/vol), left overnight at 4 °C, and filtered twice. After, cells were washed three times with distilled water. To assess the lipid accumulation, the ORO dye, which was retained in the cells, was eluted with l mL/well isopropanol, and quantified by measuring the OD at 510 nm using a spectrophotometer. The results are expressed relative to control cells (Ferrante et al. 2014).

3.5.3. Cellular oxygen consumption measurement

HepG2 cells were seeded in Seahorse XFp Analyzer (Agilent Technologies, Santa Clara, CA, USA) in mini plates at 30.000 cells/well in RPMI growth medium overnight. Cells were treated with the tested compounds as previously described; then, the medium was replaced with 750 µl unbuffered Seahorse XF Base medium supplemented with glucose (10 mM), L-glutamine (2 mM), sodium pyruvate (1 mM), equilibrated at 37°C in a CO2-free incubator for 1 h, following manufacturer's instructions. Respiration was expressed as oxygen consumption rate (OCR, pmol/min). The proton leak was determined after inhibition of mitochondrial ATP production by 1 µM oligomycin (as an inhibitor of the F0/F1 ATPase). Afterward, the mitochondrial electron transport chain was maximally stimulated by the addition of the uncoupler FCCP (2 µM). The extra-mitochondrial respiration was estimated after the injection of rotenone (1 µM) and antimycin A (0,5 µM), inhibitors of the complexes I and III, respectively. Coupling efficiency is the proportion of the consumed oxygen to drive ATP synthesis compared with that driving proton leak (% of ATP-linked OCR/basal OCR). OCR was normalized to the protein content of each well for all measurements by Bradford assay (Divakaruni et al. 2014).

3.5.4. Adipogenic differentiation and cell treatment

3T3-L1 mouse fibroblast cells, purchased from European Collection of Animal Cell Cultures (Salisbury, Wiltshire, U.K.), were maintained in standard Dulbecco's modified Eagle's medium (DMEM) supplemented with 10% FBS and 100 U/mL penicillin and 100µg/mL streptomycin. Cultured cells were grown at 37°C in a humidified 5% CO2 atmosphere with media changes every 2–3 days. The standard procedure of adipogenic

differentiation is shown in ***Fig. 4.5.4.1***. At the confluence (ID 0), the cells were incubated in DMEM containing 10μM of dexamethasone (DEX), 0.5 mM of 3-Isobutyl-1-methylxanthine (IBMX), 10μg/mL of insulin (INS) and 10% FBS for 2 days (ID 2), defined as the adipogenesis-inducing medium. Then cells were cultured in adipogenesis maintaining medium (DMEM containing 10μg/mL INS and 10% FBS) for 2 days (ID 4), followed by DMEM with 10% FB for another 3 days (ID 7) (Ferrante et al. 2014). At days 8-10, mature adipocytes were pre-treated with PEA (1μM). After 2-hours of pre-incubation, cells were insulted with Pal 300 μM. At the end of experimental period (24 hours), cells were harvested. Relative lipid content was measured as previously described. In another set of experiment, mature adipocytes were pretreated with PEA and GW6471(5 μM), a PPAR-α antagonist, insulted with Pal as well and challenged with isoproterenol (ISO, 100 μM) for 6 hours, in order to activate thermogenesis. Then, cells were lysed, and total protein fraction was extracted for following analysis.

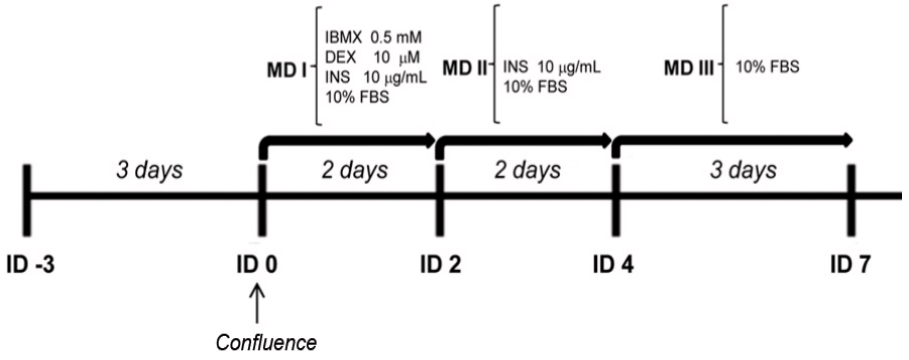

Figure 3.5.4.1. 3T3-L1 differentiation protocol. Cells were seeded to reach confluence at ID 0, after 48 hours, fibroblast were incubated with media supplemented of DEX; IBMX and INS. At days 8-10, mature adipocytes were stimulated with PEA and GW6471, and challenged with Pal.

3.5. Statistical Analysis

Data are presented as mean value ± SEM. Statistical analysis was performed by one- or two-way ANOVA followed by Bonferroni's post-hoc, for multiple comparisons. Differences among groups were considered significant at values of $P<0.05$; different superscripted letters indicate significant statistical differences.

Analyses were performed using GraphPad Prism 7 (GraphPad Software, San Diego, CA, USA).

4. Results Section

4.0. PEA counteracts hepatic metabolic inflexibility modulating mitochondrial function and efficiency in HFD-induced obese mice

4.1. PEA reduced lipid accumulation, increased energy expenditure and resting metabolic rate

The mean body weight of all groups was reported, starting 12-week after HFD feeding throughout the 8-week treatment (***Fig. 4.1.1. A***). PEA treatment gradually reduced body weight, reaching significance after 7 weeks. Consistently, 8-week treatment with PEA reduced fat mass (***Fig. 4.1.1. B***). Total energy intake of HFD+PEA group was lower than that of HFD (***Fig. 4.1.1. C***). Interestingly, PEA treatment increased energy metabolism, as shown by the higher VO_2 consumption and VCO_2 production compared to HFD mice (***Fig. 4.1.1. D***). Notably, RQ ratio decreased in PEA-treated HFD mice (RQ < 0.7) indicating an increase in FAO (***Fig. 4.1.1. E***). Consistently, the energy expenditure of HFD+PEA mice was increased compared to HFD ones (***Fig. 4.1.1. F***).

4.2 PEA modulated circulating levels of hormonal and inflammatory parameters

In ***Table 4***, biochemical and hormonal parameters are reported. Serum triglycerides, cholesterol, ALT, and TNF-α increased by HFD, were significantly reduced by PEA. Similarly, the hormonal profile altered by

HFD was improved by PEA treatment, as shown by leptin and adiponectin serum levels, whose ratio was consistently reduced.

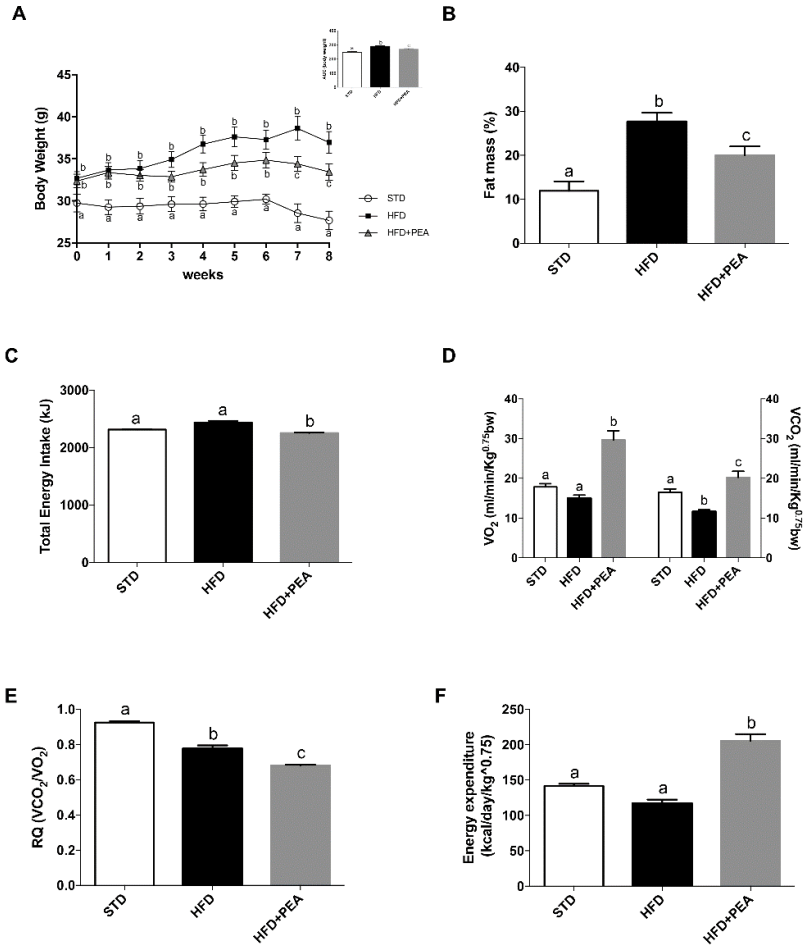

Figure 4.1.1. PEA reduced body weight and increased energy expenditure in diet-induced obese mice. (***A***) Effect of PEA treatment on body weight measured throughout the treatment period (0-8 weeks after 12-week HFD feeding), (**B**), Fat mass measured by bioelectrical impedance analysis and (**C**), Total energy intake was obtained considering weekly food intake and dietary gross density energy (n = 10 each group). (**D**), VO2 consumption and VCO2 production, (**E**), RQ (VCO2/VO2), (**F**), Energy expenditure was determined at the end of experimental period by an open-circuit calorimeter (n = 5 each group). Data are presented as means ± SEM. Labeled means without a common letter differ, $P<0.05$

	STD	HFD	HFD + PEA
Triglycerides (mg/dL)	116.1 ± 5.124^{a}	213.6 ± 3.618^{b}	151.2 ± 4.505^{c}
Total Cholesterol (mg/dL)	163.7 ± 4.479^{a}	227.6 ± 4.694^{b}	190.9 ± 2.489^{c}
Serum ALT (U/L)	70.14 ± 2.064^{a}	124.1 ± 3.894^{b}	98 ± 4.416^{c}
Serum TNF-α (ng/mL)	0.9514 ± 0.0504^{a}	3.777 ± 0.1205^{b}	1.202 ± 0.2694^{a}
Leptinemia (ng/µL)	1.29 ± 0.0626^{a}	18.4 ± 0.9042^{b}	14.77 ± 0.4992^{c}
Adiponectinemia (µg/mL)	3.099 ± 0.08055^{a}	1.19 ± 0.09502^{b}	2.688 ± 0.1893^{a}
Ratio (leptin/adiponectin)	0.4185 ± 0.02418^{a}	16.09 ± 1.516^{b}	5.702 ± 0.6046^{c}
Insulin (ng/dL)	0.394 ± 0.01451^{a}	1.545 ± 0.5375^{b}	0.4443 ± 0.0321^{a}
Glucose (mg/dL)	93.5 ± 3.794^{a}	135.4 ± 6.871^{b}	102.5 ± 90.31^{a}
HOMA index	1.744 ± 0.04303^{a}	5.646 ± 1.467^{b}	2.783 ± 0.3655^{c}

Table 4. Biochemical and hormonal parameters. Data are expressed as mean ± SEM (n = 6 for each group). Labeled mean without a common letter differ, $P< 0.05$.

4.3. PEA reduced liver damage and improved hepatic lipid metabolic impairment

The histological pattern of HFD mice was characterized by micro- and macro-vesicular steatosis with prominent ballooning. Lobular inflammation was characterized by inflammatory cells occasionally arranged in microgranulomas (see arrow) and consisting mostly in lymphocytes, plasma cells, and neutrophils (***Fig. 4.3.1 A***). Liver sections of HFD+PEA animals showed a mild reduction of zone 1 micro-vesicular steatosis and ballooning, accompanied by a reduction of inflammatory lesions and absence of necrosis (***Fig. 4.3.1 B***). Moreover, PEA reduced hepatic lipid accumulation caused by HFD feeding, as shown by the slight positivity to ORO staining (***Fig. 4.3.1 A***). Accordingly, the increase in hepatic triglycerides of HFD mice was reduced by PEA treatment (***Fig. 4.3.1 C***). Furthermore, PEA

increased *Ppara* and reduced *Fas*n transcription (***Fig. 4.3.1 D***), associated to increased phosphorylation of AMPK and its downstream target ACC (***Fig. 4.3.1 E, F***), the main pathway involved in FAO.

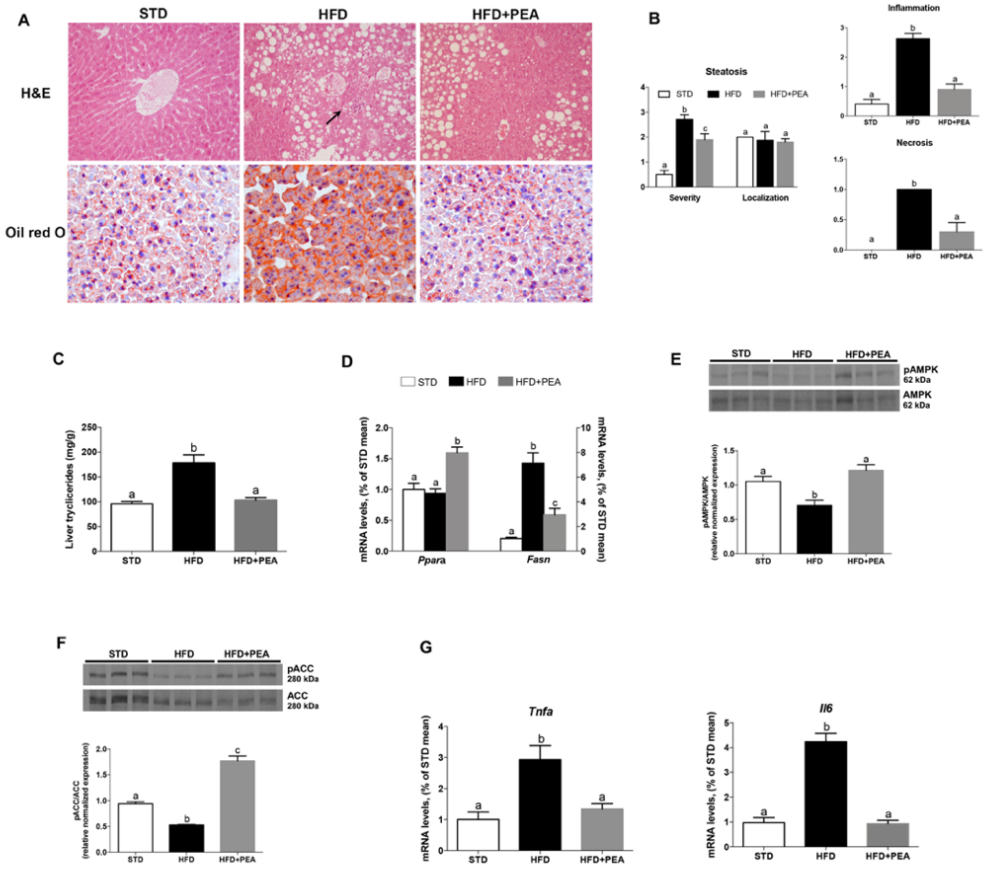

Figure 4.3.1. PEA effect on liver lipid accumulation in HFD-fed mice. (***A***), Paraffin-embedded sections of the liver (n = 4 each group) were stained with H&E and Oil Red O. Micrographs are representative pictures with original magnification ×20. (***B***), Effect of PEA treatment on severity of steatosis, hepatic inflammation, and necrosis was also evaluated by Kleiner's grading system. (***C***), Liver triglycerides content, (***D***), *Ppara* and *Fasn* mRNA levels, (***E***), Liver pAMPK-to-AMPK, (***F***), pACC-to-ACC were evaluated by Western blot and densitometric analysis shown. (***G***), *Il6* and *Tnfa* mRNA level are reported. Data are presented as means ± SEM of animals from different groups (n = 4-6 each group). Labeled means without a common letter differ, $P<0.05$

To further confirm the involvement of PPAR-α pathway in PEA-mediated effect, Western blot analysis was performed to evaluate protein expression of PPAR- α, its coactivator PGC1 α, and the downstream target CPT1. As reportedin ***Fig 4.3.2 (A, B)***, PEA increased the expression of these mediators, demonstrating that hepatic PEA effects were mainly mediated by PPAR-α activation. Based on the extended hepatic inflammation grade of HFD mice, we explored *Il6* and *Tnfa* mRNA expression, two inflammatory mediators implicated in the pathogenesis of steatosis and IR. PEA-treated HFD mice showed a reduction in both cytokine transcription levels, confirming PEA anti- inflammatory profile in HFD-induced steatosis (***Fig. 4.3.1 G)***.

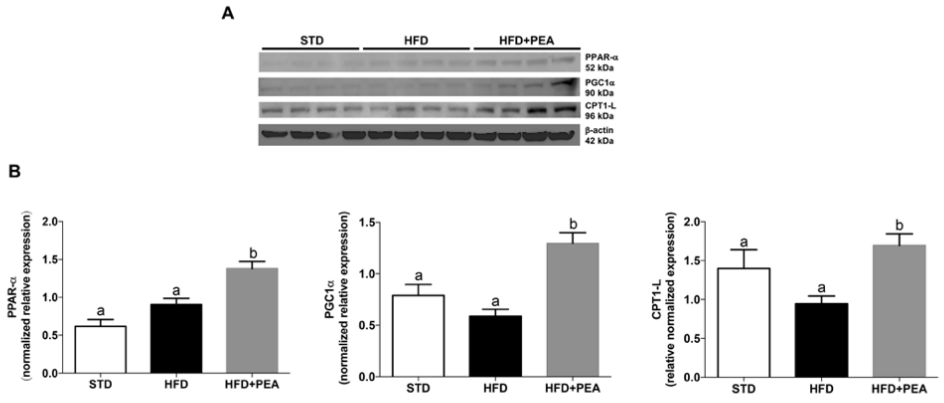

Figure 4.3.2. PEA induced PPAR-α and PGC1α expression in HFD mice. (***A***), In liver, protein expression of PPAR-α, the co-activator PCG1α, and its downstream target CPT1-L was evaluated and (**B**), densitometric analysis was reported. Data are presented as means ± SEM of animals from different groups (n = 4-6 each group). Labeled means without a common letter differ, $P<0.05$.

4.4. Determination of PEA and long-chain fatty acids in mouse liver

In order to evaluate whether the excess of fat deposition in the liver of mice feeding fat diet was influenced by PEA levels, PEA level and those of some

long-chain fatty acids (i.e. palmitic, palmitoleic and oleic acids) were measured in the liver. Notably, HFD decreased significantly hepatic PEA levels, that were normalized by PEA oral treatment. Palmitic acid levels were strongly altered by HFD, but unchanged in HFD+PEA animals; however, palmitoleic acid and oleic acids were slightly reduced in PEA treated animals (***Table 5***).

	STD	HFD	HFD + PEA
PEA (pmoles/g tissue)	24.824 ± 2.873^{a}	11.432 ± 0.562^{b}	22.796 ± 1.840^{a}
Palmitic Acid (16:0) (µmoles/g tissue)	35.228 ± 1.911^{a}	44.614 ± 4.326^{b}	44.654 ± 4.448^{b}
Palmitoleic acid (16:1) (µmoles/g tissue)	2.723 ± 0.496^{a}	6.042 ± 0.810^{b}	4.219 ± 0.528^{b}
Oleic acid (18:1) (µmoles/g tissue)	12.794 ± 1.577^{a}	39.350 ± 6.395^{b}	32.423 ± 3.720^{b}

Table 5. Determination of PEA and long-chain fatty acids (palmitic, palmitoleic, and oleic acids) in mouse liver. Data are presented as means ± SEM of animals from different groups (n = 4-6 each group). Labeled means without a common letter differ, $P<0.05$

4.5 Modulation of hepatic mitochondrial efficiency and oxidative stress by PEA treatment

In our experimental condition, liver from HFD mice displayed an altered expression of mitochondrial dynamic-related protein compared to STD mice. Chronic high fat feeding resulted in an increased of MFN2 and a reduction of DRP1 protein expression, suggesting the onset of stress-related defensive mechanisms (***Fig. 4.5.1 A-B***) (Lopez-Lluch 2017). PEA-treatment restore MFN2 and DRP1 protein expression, also increasing FIS1

level (***Fig. 4.5.1 A, B***). These results lead us to assume a possible involvement of PEA in re-establishing and managing mitochondrial health.

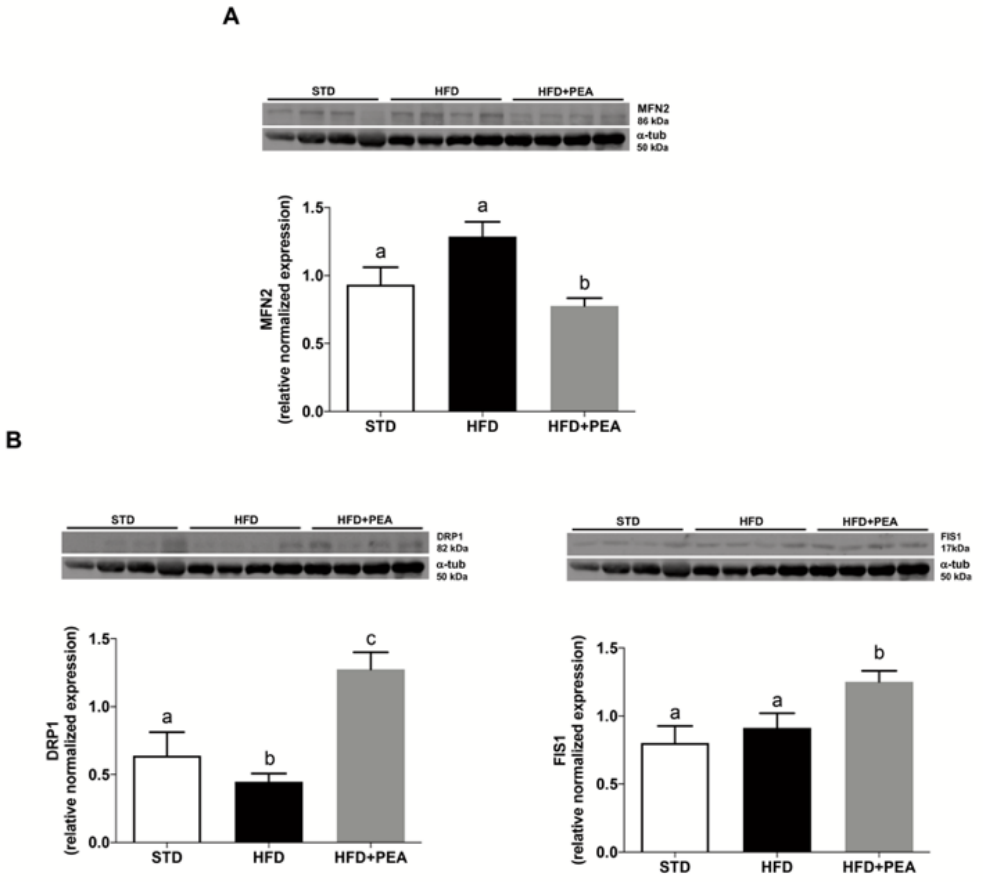

Figure 4.5.1 PEA recovered the unbalanced mitochondrial dynamics in HFD mice. Western blot analysis of MFN2 (***A***), DRP1 and FIS1 (***B***) in liver from STD, HFD and HFD+PEA is reported. Data are presented as means ± SEM of animals from different groups (n = 4-6 each group). Labeled means without a common letter differ, $P<0.05$.

To confirm the involvement of PEA-effect on mitochondrial function, hepatic mitochondrial respiration was evaluated in isolated organelles from the mice of all experimental groups (***Fig 4.5.2.***).

Mitochondrial state 3 respiration, evaluated using succinate as substrate, was decreased in HFD-fed animals compared with the other groups and restored by PEA ***(Fig 4.5.2 A)***. To study FAO, state 3 respiration was measured using palmitoyl-carnitine as substrate; PEA increased oxygen consumption compared with STD and HFD groups ***(Fig 4.5.2 B)***. No variation was observed in mitochondrial state 4 respiration among all groups using succinate or palmitoyl-carnitine substrate ***(Fig 4.5.2 A, B*** respectively). High quality of mitochondrial preparations was indicated by high respiratory control ratio values in all groups (data not shown). CPT activity did not differ between STD and HFD fed mice, while it was increased by PEA treatment ***(Fig 4.5.2 C)***. To test mitochondrial efficiency, we measured oxygen consumption in the presence of oligomycin and FCCP ***(Fig 4.5.2 D)***. Oligomycin state 4 respiration showed a significant reduction in HFD animals compared to STD, whereas it was significantly increased in PEA-treated mice ***(Fig 4.5.2 D)***. No variation was found in maximal FCCP-stimulated respiration ***(Fig 4.5.2 D)***. Therefore, hepatic mitochondrial energetic efficiency, assessed as the degree of coupling, was increased in HFD and decreased by PEA treatment ***(Fig 4.5.2 E)***. This reduction in energy efficiency is associated to PEA-induced increase in mRNA expression of uncoupling protein (UCP)2 ***(Fig 4.5.2 F)***. UCP2 is an anion transporter involved in mitochondrial calcium homeostasis and is related to the increase in proton leak and the reduction of ROS production (Mailloux and Harper 2011). Hepatic ROS production, increased in HFD mice, was significantly decreased by PEA (**Fig. 4.5.3. *A***). Accordingly, PEA increased antioxidant defence, promoting SOD, aconitase, and catalase activity (**Fig. 4.5.3. *B-D***). Moreover, the hepatic GSH level was reduced by HFD and

increased by PEA treatment, and no difference in GSSG content was shown among groups (**Fig. 4.5.3. *E***).

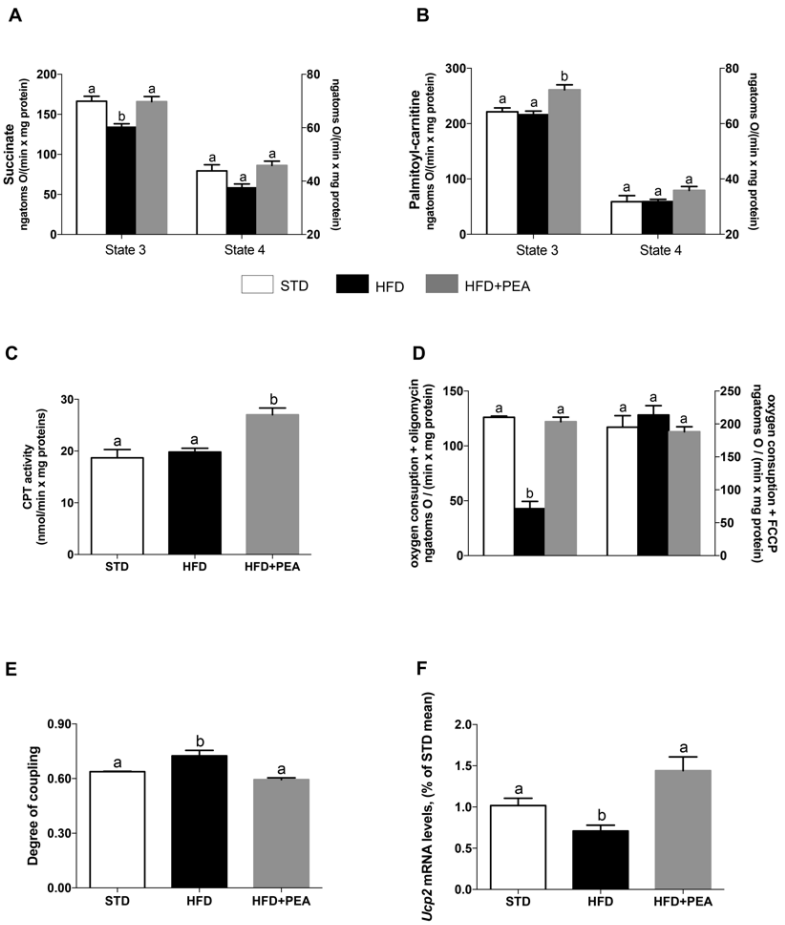

Figure 4.5.2. Effect of PEA on liver mitochondrial function and energy efficiency. (**A**), Mitochondrial respiration in presence of succinate or (***B***), palmitoyl-carnitine, as substrates, was determined in presence of ADP (state 3) and in the presence of substrates alone (state 4). (**C**), CPT activity was determined in isolated liver mitochondria. The oxygen consumption rate was evaluated (**D**), In the presence of oligomycin, that inhibits ATP synthase, and FCCP, which dissipates trans-mitochondrial proton gradient. (***E***), the degree of coupling is also shown. (F), mRNA levels of UCP2 were also reported. Data are presented as means ± SEM of animals from different groups (n = 4-6 each group). Labeled means without a common letter differ, $P<0.05$.

The beneficial effects on liver redox status induced by PEA were clearly indicated by the significant increase of the GSH/GSSG ratio (**Fig. 4.5.3. *F***).

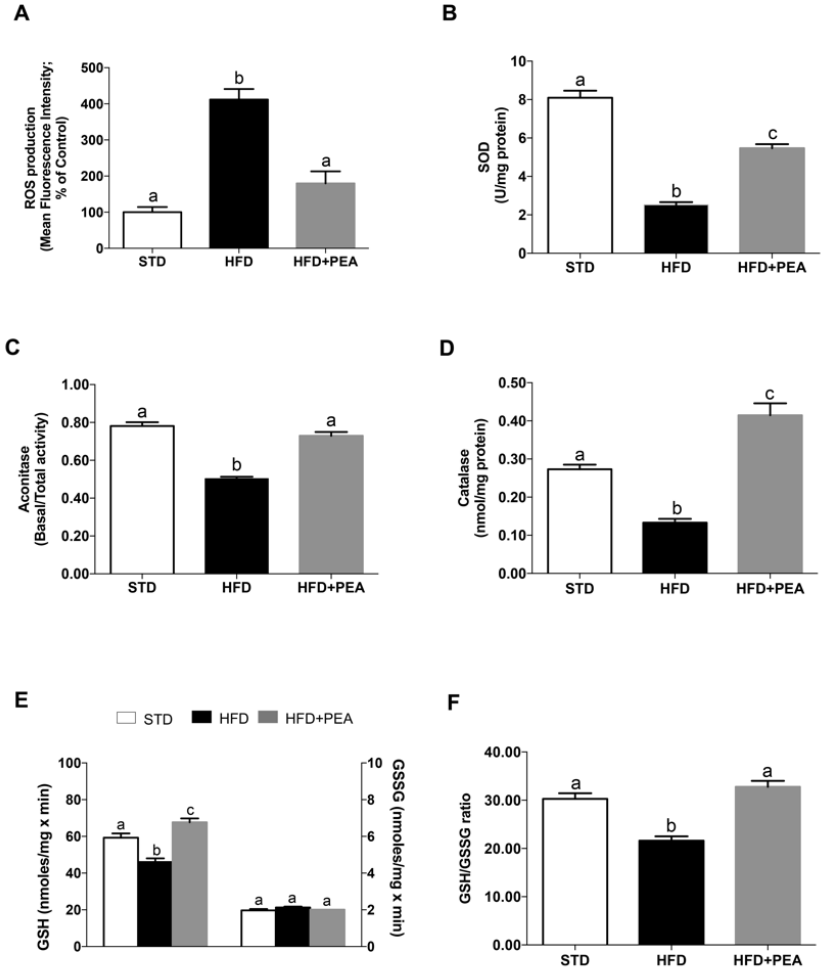

Figure 4.5.3. PEA improves antioxidant/detoxifying defense in liver of HFD-fed mice. (***A***), ROS production, (***B***), SOD, (***C***), Aconitase, (***D***), Catalase activity is reported. (***E***), GSH and GSSG content, and (***F***), The GSH-to-GSSG ratio are shown. Data are presented as means ± SEM of all animals from different groups (n = 6 each group). Labeled means without a common letter differ, $P<0.05$

4.6. PEA counteracts mitochondrial dysfunction in palmitate challenged HepG2 cells

PEA effect on mitochondrial bioenergetics in Pal-treated cells was assessed using MitoStress assay by Seahorse analyzer (***Fig. 4.6.1. A***) resembling steatosis and IR *in vitro*. PEA treatment recovered Pal-induced mitochondrial dysfunction, increasing basal and maximal respiration (***Fig. 4.6.1. B, C***) promoting ATP-linked respiration and proton leak (***Fig. 4.6.1. D, E***), and reducing mitochondrial coupling efficiency (***Fig. 4.6.1. F***). All these data indicate the direct effect of PEA in counteracting Pal-induced mitochondrial dysfunction.

4.7. Involvement of AMPK in PEA effect on lipid metabolism in HepG2 cells

The *in vivo* findings suggest the possible involvement of AMPK in PEA mechanism of action. To demonstrate this hypothesis, we designed *in vitro* experiment using compound C, a potent inhibitor of AMPK.

The direct lowering effect of PEA on hepatic lipid accumulation induced by Pal was shown on HepG2 cells (***Fig. 4.7.1. A***). Notably, the PEA effect was blunted by compound C (***Fig. 4.7.1. A***). In fact, PEA restored AMPK phosphorylation and increased PPAR-α and CPT1 expression in Pal-challenged HepG2 (***Fig. 4.7.1. B***) and all these effects were reversed in the presence of compound C (***Fig. 4.7.1. C)***, clarifying the key role of AMPK in PEA metabolic activity.

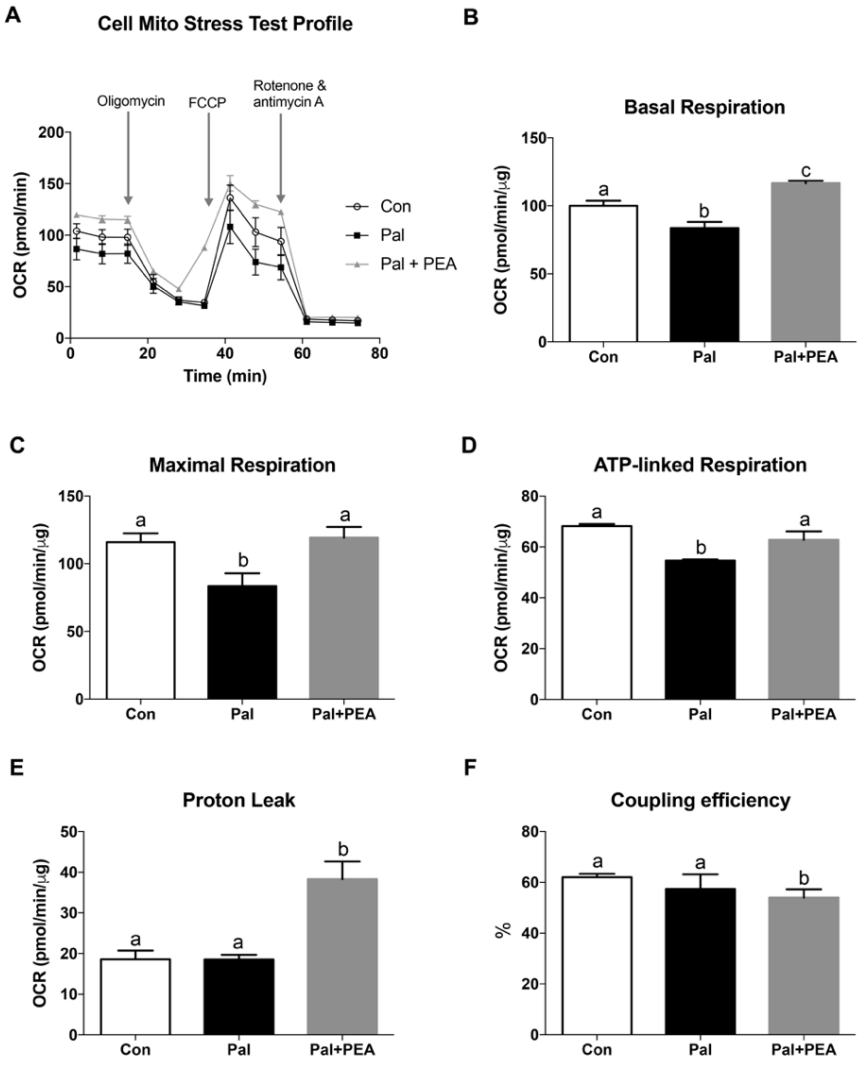

Figure 4.6.1. PEA effect on mitochondrial function of Pal-challenged HepG2 cells. (***A***), Basal oxygen consumption rate (OCR) was determined by Cell Mito Stress Test in Sea Horse analyzer, following the addition of oligomycin, the uncoupler FCCP, rotenone and antimycin A, inhibitors of complexes I and III, respectively. (***B***), Basal respiration, (**C**), maximal respiration, (***D***), ATP-linked respiration, (***E***), proton leak, as well as ***F***, coupling efficiency were calculated in HepG2 cells stimulated with Pal (100 μM) in presence or not of PEA (1 μM). OCR was normalized to the protein content of each well for all measurements by Bradford assay. Data are the mean ± SEM of three different experiments with three technical replicates. Labeled means without a common letter differ, $P<0.05$

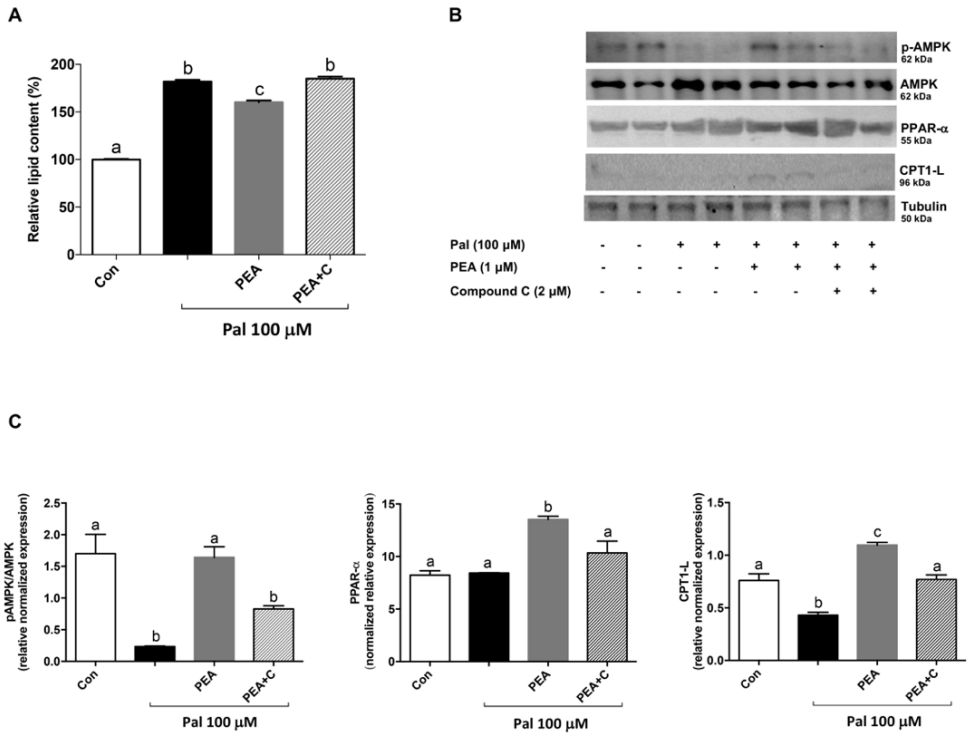

Figure 4.7.1. Involvement of AMPK in PEA effect on lipid metabolism in HepG2 cells. A, Lipid content was assessed in Pal-challenged HepG2 cells, treated or not with PEA or compound C, an inhibitor of AMPK. B, Protein expression of pAMPK-to-AMPK, PPAR-α, CPT1 was reported. C, Densitometric analysis of pAMPK-to-AMPK, PPAR-α, CPT1 was also determined. Data are from three different experiments in duplicate and presented as means ± SEM. Labeled means without a common letter differ, $P<0.05$

5.0. Brown adipogenic reprogramming by PEA in HFD-induced obese mice.

5.1. PEA promotes a rearrangement of BAT morphology and activity and reduces adipocytes hypertrophy in scWAT

H&E staining of iBAT demonstrated that in obese mice brown adipocytes were deeply converted from multilocular to paucilocular/unilocular phenotype (***Fig 5.1.1.***). Interestingly, PEA-treated animals exhibited a mild recovery of the brown-like phenotype, characterized by the appearance of several adipocytes and a typical multilocular lipid droplet arrangement. The increased multilocularity observed in PEA-treated animals matched with an increased UCP1 immunohistochemical staining, suggesting that PEA treatment was able to reconvert the inhibited and whitened brown adipocytes of obese mice to a more functional state (***Fig 5.1.1.***).

It is well known that iBAT morphology and function is sustained by an extended parenchymal sympathetic noradrenergic innervation (Murano I et al). Therefore, to further assess the effects of PEA on BAT, TH immunohistochemistry serial sections was performed. Morphometric data showed an increased density of noradrenergic nerves in iBAT of PEA treated mice (***Fig. 5.1.2.***).

In inguinal fat depots, HFD mice exhibited a significant hypertrophy of adipocytes compared to control. Despite no significant differences was found in *de novo* adipogenesis transcriptional level (***Fig 5.2.2.***), H&E staining of HFD+PEA revealed a reduction in adipocytes size and area, as shown in ***Fig 5.1.3.*** (A and B).

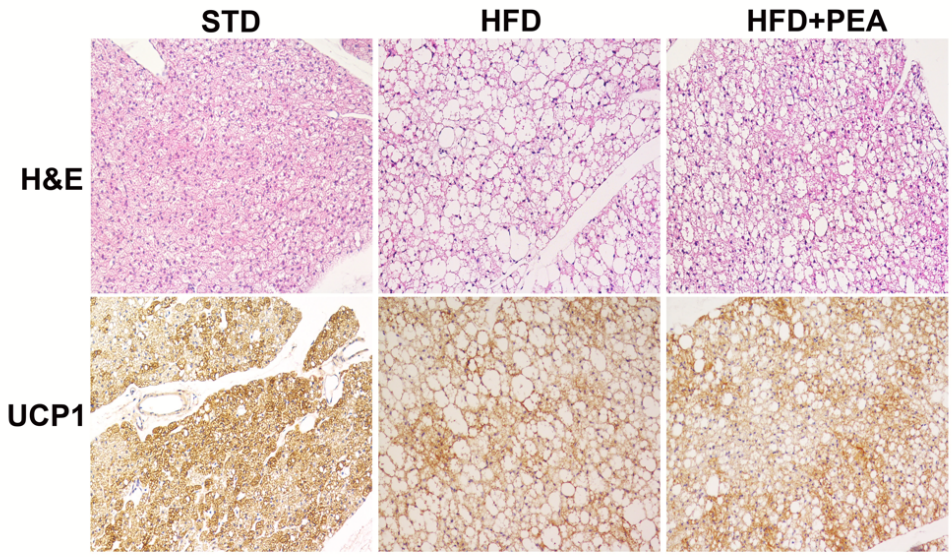

Figure 5.1.1. Morphological staining of iBAT. In Panel A, paraffin-embedded alternate sections were stained with H&E. Immunohistochemical staining for UCP1 reveals total protein tissue expression. Original magnification 20X.

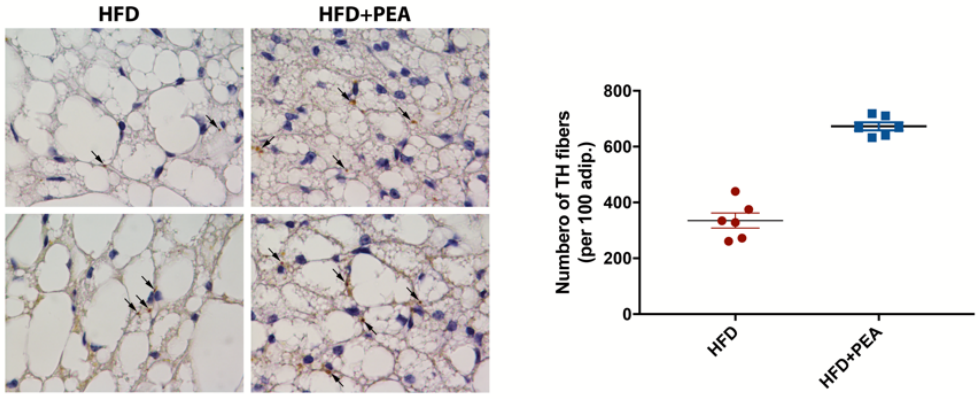

Fig 5.1.2. Immunohistochemistry staining for TH in iBAT. Representative staining of TH antibody is reported, and the total count of positive fibers were performed in a double- blinded manner (n=7 animals for each group). Original magnification 100X.

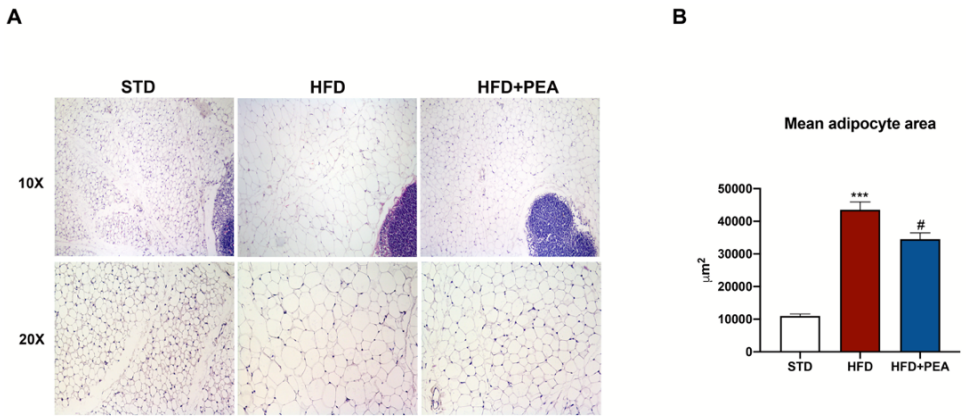

Figure 5.1.3. PEA effect on adipocytes hypertrophy. A, H&E of scWAT from STD, HFD, HFD+PEA mice. Magnification 10X and 20X and B, mean of adipocyte size.

5.2. PEA effects on thermogenic marker in BAT and scWAT

At molecular level, iBAT from HFD animals displayed an altered brown phenotype, with reduced gene expression of *Ucp1*, *Ppargc1a*, *Prdm16*, *Cox8b*. PEA significantly induced expression of brown thermogenic genes in iBAT (***Fig.5.2.1***). PEA also modulates browning phenomenon in scWAT, the main fat pad responsive to thermogenic stimuli. Indeed, PEA increased gene expression of *Ucp1*, *Prdm16* and *Ppargc1a*, without affecting *de novo* adipogenesis, as demonstrated by no modification in Fabp4 mRNA level in HFD and HFD+PEA (***Fig.5.2.2. A***).

Furthermore, PEA recovered the phosphorylation of AMPK and the protein expression of PGC1α in scWAT, reduced by HFD (***Fig.5.2.2. B***), suggesting the beige adipocyte transdifferentiation induced by PEA.

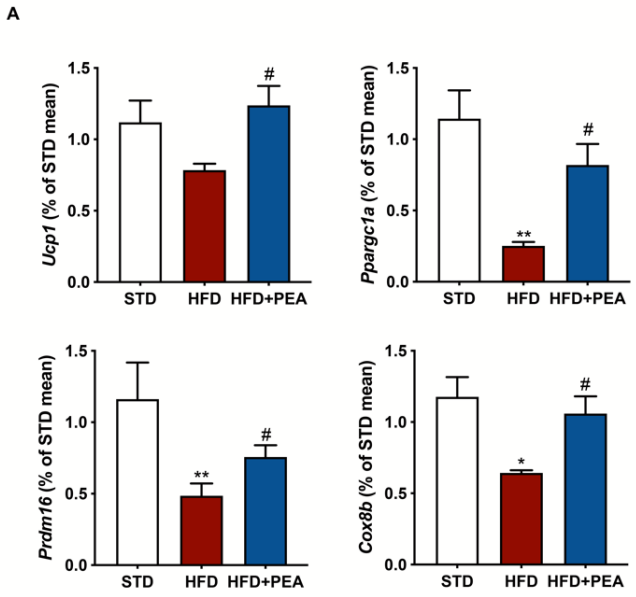

Figure 5.2.1. PEA induces transcription of thermogenic marker in BAT of HFD mice. Result are shown as mean ± SEM (*P<0.05, **P<0.01 vs STD; #P<0.05, vs HFD)

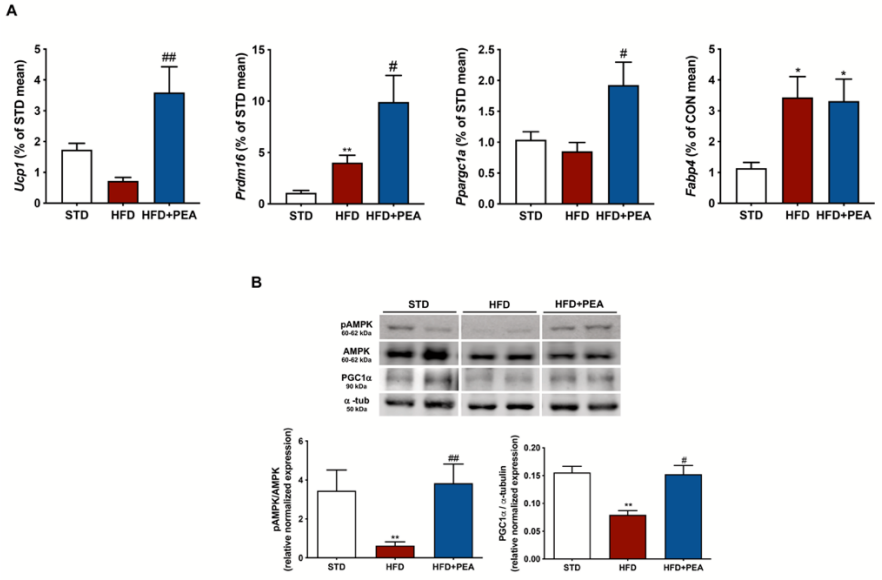

Figure 5.2.2. PEA manage beige adipocyte metabolism in scWAT. A, In HFD+PEA mice, an increase in Ucp1, Prdm16, Ppargc1a gene expression were demonstrated. Moreover, PEA induced an increased protein expression of phospho-AMPK and PGC1α compared to HFD mice. Result are shown as mean ± SEM (*P< 0.05, **P< 0.01 vs STD; #P< 0.05, ##P< 0.01 vs HFD);

5.3. PEA restore leptin signaling pathway, providing endocrine and immune regulation in scWAT of HFD animals

The significant reduction of circulating leptin level (***Table 4***), prompt us to explore the involvement of leptin signaling pathway in PEA endocrine and anti-inflammatory effects. In obese animal the dramatic increased of leptin serum level is accompanied by a reduction of STAT3 phosphorylation and an increase of the inhibitory SOCS protein expression, demonstrating an impairment of leptin signaling pathway that underlines the peripheral leptin resistance in adipose tissue. As shown in ***Fig 5.3.1.*** PEA restored both phospho-STAT3 and SOCS protein expression, improving leptin sensitivity in scWAT.

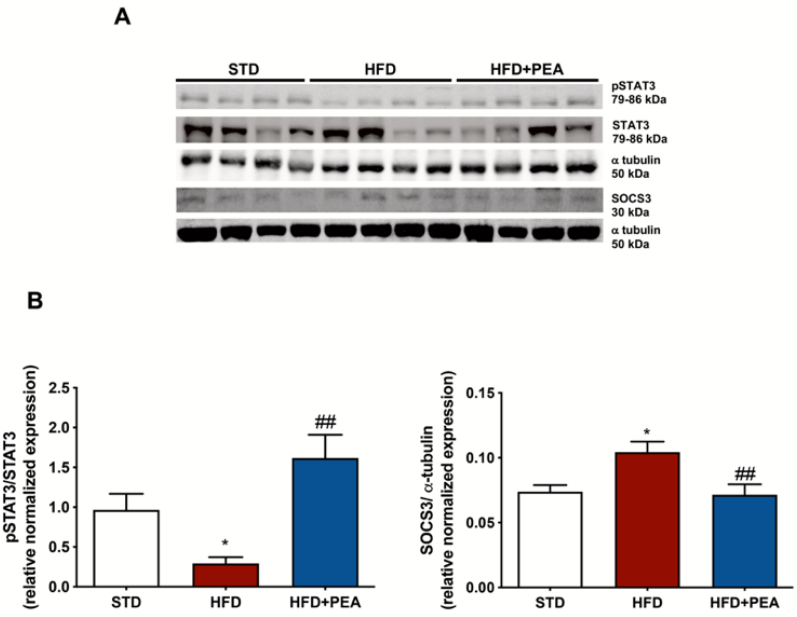

Figure 5.3.1. PEA effect on leptin signaling pathway in scWAT. A, Leptin signaling pathway was evaluated by Western blot analysis in inguinal fat depots. **B** Densitometric analysis of pSTAT3-to STAT3 and SOCS3 was also reported. Result are shown as mean ± SEM (#P<0.05, vs STD; **P<0.01, ***P< 0.001 vs HFD).

Since chronic inflammation of WAT occurs during obesity, we evaluated the effect of PEA on subcutaneous adipose tissue inflammation. In HFD mice, gene expression of *Tnfa* and *Il-6* was strongly up-regulated (***Fig 5.3.2. A***), while *Il-10, Adipoq* and *Pparg* mRNA levels reduced (***Fig 5.3.2 B***). Interestingly, PEA reduced obesity-related inflammation, decreasing pro-inflammatory cytokine (i.e. TNF and IL-6) and increasing anti-inflammatory cytokines (IL-10) and adipokines (adiponectin) and increasing PPAR-γ gene expression (***Fig 5.3.2.***).

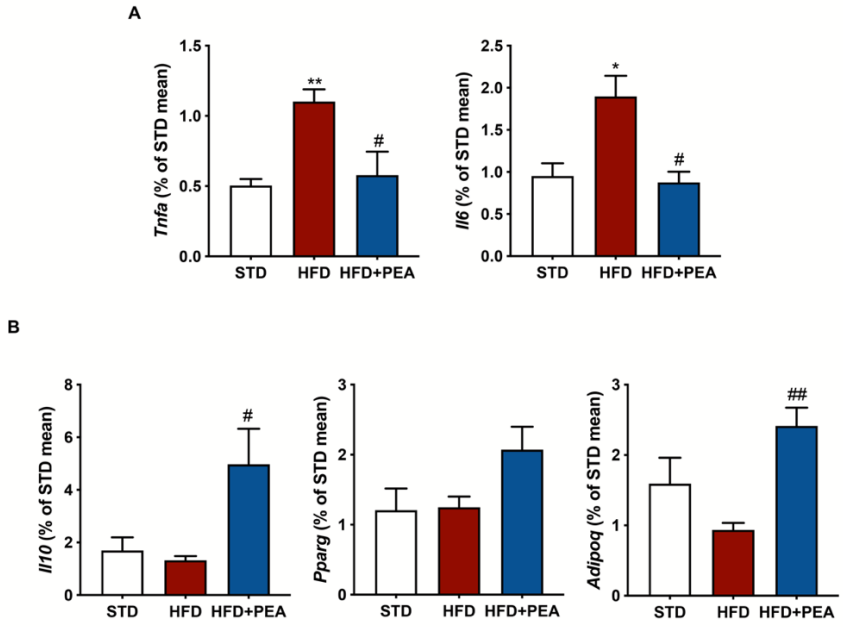

Figure 5.3.2. PEA reduce inflammation in scWAT of obese mice. A, *Tnfa* and *Il-6* and **B**, *Il10*, *Adipoq*, *Pparg* mRNA level are reported. Results are shown as mean ± SEM (*P<0.05, **P< 0.01 vs STD; #P<0.05 vs HFD).

5.4. PEA activates AMPK signaling pathway in 3T3-L1 mature adipocytes.

To clarify the mechanism of action by which PEA exerts its beneficial effect in adipocyte, we used an *in vitro* experimental model.

In mature adipocytes exposed to Pal, 24-hours treatment of PEA markedly normalized lipid content, as showed in ***Fig 5.4.1***.

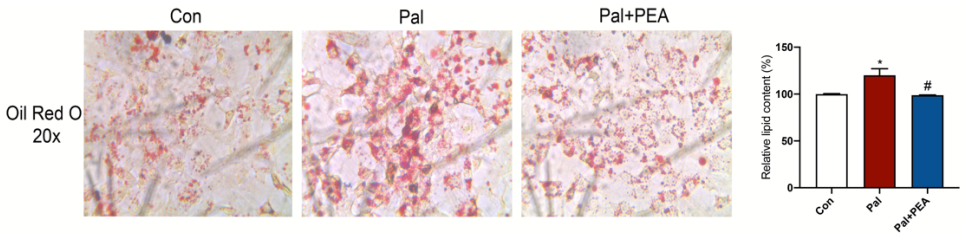

Figure 5.4.1. PEA increased thermogenic activation in mature adipocytes. Oil Red O staining revealed an increased lipid accumulation in Pal group, reduced in PEA-treated cells (*P<0.05 vs Con; #P<0.05 vs Pal).

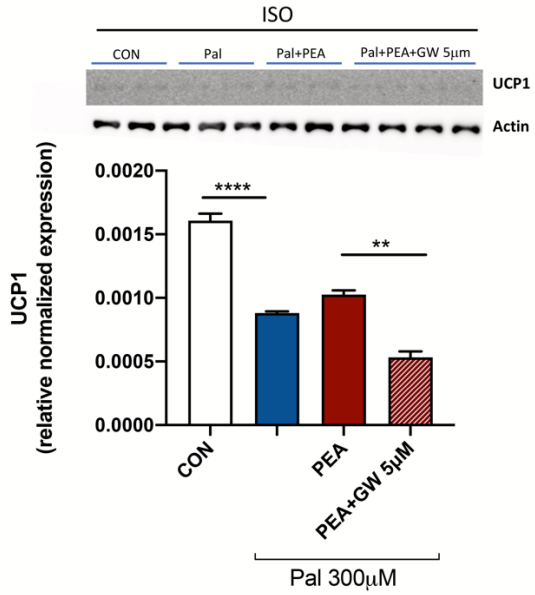

Figure 5.4.2. PEA increased UCP1 protein expression in ISO-challenged 3T3-L1. After differentiation, 3T3-L1 were stimulated with PEA (1µM) and GW6471 (5µM) and insulted with Pal (300 µM). 6 hours before the washout, cells were challenged with the β3-agonist isoproterenol (ISO, 100 µM) to activate lipolytic and thermogenic features of adipocytes (**p < 0.01; ****p<0.0001).

Interestingly, in ISO-challenged adipocytes, PEA promoted UCP1 protein expression, impaired by Pal. According to our hypothesis, GW6471 pre-treatment, a potent PPAR-α antagonist, dampened PEA effect on UCP1 expression, suggesting a possible PPAR-α dependent mechanism in PEA-stimulated thermogenic pathway, on hypertrophic adipocytes (***Fig.5.4.2.***)

6. Discussion and Conclusion

The identification of PPARs and their ligand led to the discovery of the direct role of lipids in modulation of the gene expression. Specifically, PPAR-α act as a crucial regulator of whole-body homeostasis, ipid and glucose metabolism, therefore it can be considered an intriguing target for NAFLD therapy (Desvergne and Wahli 1999). Unfortunately, the weak safety profile of the available PPAR-α agonist, the fibrates, claimed the requirement of novel efficient and safe agents (Tanaka et al. 2017).

Rodriguez de Fonseca et al. (2001)demonstrated that OEA, an endogenous NAEs, caused a profound decrease in food intake and body weight and lately, it was demonstrated that OEA suppressive effect on appetite was attributed to its interaction with PPAR-a receptor (Fu et al. 2003, Nielsen et al. 2004, Laleh et al. 2018). Recently, its anorectic effect and hepatoprotective properties have been reviewed (Tutunchi et al. 2019). In many other studies, OEA treatment showed not only hepatoprotective and lipolytic effect in adipose tissue, but also exhibited anti-inflammatory properties via PPAR-α activation (Guzmán et al. 2004, Suarez et al. 2014, Chen et al. 2015, Tutunchi et al. 2019).

In this study, we determined the modulatory effect of PEA, a congener of OEA belonging to N-acylethanolamine family, on hepatic metabolic inflexibility and adipose tissue remodeling in an animal model of diet-induced obesity. As mentioned above, the main PEA effects are due to its interaction with PPAR-α (Lo Verme et al. 2005, Mattace Raso et al. 2014).Therefore, during the first year of my PhD program, the research was focused on the evaluation of PEA metabolic effect in an in vivo model of

diet-induced obesity. PEA limited overweight and adiposity induced by HFD, reducing energy intake, increasing energy expenditure, resting metabolic rate, and lipid oxidation, as shown by the reduced RQ. Indeed, the decreased RQ index reflects the preferential cellular use of fatty acids rather than carbohydrate, dissipating most part of energy gained from HFD. In obese mice, the increased lipid oxidation induced by PEA determines an improvement of lipid and inflammatory profile, limiting the progression of hepatic steatosis in NASH.

Recently, the activation of AMPK, a cellular energy sensor, has been identified as a therapeutic target for treating metabolic diseases (Day et al. 2017). The activation of this sensor leads to the phosphorylation of key metabolic mediators and transcriptional regulators, including PPARs, that are linked to cellular metabolism (Herzig and Shaw 2018). Indeed, AMPK activation reprograms cells and it redirects metabolism inhibiting anabolism, increasing catabolism, limiting glucose and lipid synthesis and promoting FAO as an energy source.

Obesity and related comorbidities result from the overproduction of lipids derived by *de novo* lipogenesis and from the inability to oxidize lipids stored in the liver (Day et al. 2017). These effects are counteracted by AMPK/ACC pathway activation: in fact, the activation of AMPK reduces lipogenic gene expression, liver triglycerides, and hepatic steatosis in hyperlipidemic diabetic rats (Seo et al. 2009) and reduces lipid accumulation in hepatocytes (Zhang et al. 2016).

In our experimental conditions, PEA promotes hepatic lipid catabolism not only reducing fatty acid synthase transcription, but also directly activating AMPK signaling pathway, rescued liver capability of HFD mice in using the available lipid disposal and in managing the nutrient source gained from

diet. Furthermore, the activation of lipid catabolism leads to the reduction of hepatic ectopic lipid storage, as shown by the determination of triglyceride content and Oil Red O staining. All these effects were accompanied by an increased level of PPAR-α expression and its coactivator PGC1α, determined both *in vivo* and *in vitro*.

Previous data demonstrated that the activation of AMPK can inhibit the synthesis of proinflammatory cytokines both in macrophages (Sag et al. 2008, Yang et al. 2010) and in adipocytes (Lihn et al. 2008). Our data demonstrated that PEA treatment reduced the pro-inflammatory TNF-a and IL-6 and increased the anti-inflammatory mediators (IL-10, PPAR-g and adiponectin) in liver and adipose tissue, confirming the anti-inflammatory activity of PEA in this experimental model.

Moreover, in HFD mice PEA also improves the alterations of serum leptin and adiponectin, deeply reducing their ratio. Interestingly, it has been demonstrated that both adipokines inversely modulate glucose and lipid metabolism through AMPK signaling (Minokoshi et al. 2002, Long and Zierath 2006).

As previously demonstrated, HFD induced the disruption of mitochondrial homeostasis (Mollica et al. 2017). Here, PEA treatment modulates expression of protein involved in mitochondrial dynamics, reducing the MFN2 protein level and promote the expression of DRP1 and FIS1. All these effects reflect the PEA ability in re-balancing mitochondrial dynamics in liver of HFD mice. Moreover, the reduced mitochondrial respiratory capacity revealed a significant impairment of mitochondrial function, associated with an increased oxidative stress in liver from HFD mice. PEA improves mitochondrial respiratory capacity and FAO, decreasing mitochondrial efficiency, as shown by the degree of coupling. The recovery

of mitochondrial functionality matched with the increased transcription of UCP2, whose uncoupled activity is necessary to maintain oxidative balance in liver (Jin et al. 2013). Despite the role of UCP2 in the pathogenesis of NAFLD remain controversial, growing evidences demonstrated the protective role of UCP2 during the progression of liver and metabolic disease (Toda and Diano 2014). Concerning the oxidative stress, PEA-treated mice displayed the reduction of ROS production, the increase of aconitase, SOD and catalase activity, well-known detoxifying enzymes, as well as the reduced GSH/GSSG ratio. Moreover, it has been already described that PEA levels decreased in rat fatty liver due to overfeeding (Izzo et al. 2010) as well as in insulin-resistant obese women (Abdulnour et al. 2014); it is likely that PEA levels are affected by dysmetabolism, and that PEA biosynthesis/degradation routes may be involved in metabolic impairment. It has been reported that PEA in ultramicronized formulation is rapidly absorbed (Petrosino et al. 2018) and accordingly, the exogenous administration of PEA promoted an increase of its hepatic levels in HFD mice, whereas no change either in palmitic or palmitoleic or oleic acid content were detected. In addition, it should be considered that the amount of palmitic acid derived from PEA degradation is negligible respect to whole tissue amount and it depends on exogenous source and endogenous biosynthesis that are tightly maintained in a defined homeostatic concentration (Carta et al. 2017).

The open question remains whether PEA mediates *per se* a metabolic activity. Therefore, during the II year, the study was focused on the development of an *in vitro* model that could resemble the *in vivo* experimental condition of IR and the lipid cellular accumulation, using HepG2 cells-challenged with palmitate. In insulted HepG2 cells, the effect

of PEA on mitochondrial function showed similar results to those obtained in *in vivo* model, highlighting a direct effect of PEA on hepatocytes. PEA stimulation increased basal, maximal and ATP-linked mitochondrial respiration. Moreover, PEA exposure induced an increase in proton leak, and subsequently a reduction of coupling efficiency. The *in vitro* experiments also allowed to address the direct effect of PEA on hepatic lipid metabolism via AMPK- dependent mechanism, using compound C, a potent and selective inhibitor of the enzyme.

Pilot experiments were performed to choose PEA concentration, selecting 1 μM of PEA, the same previously used in other study on SH-SY5Y, a human neuroblastoma cell line (Avagliano et al 2016).

As known, HepG2 cells exposed to palmitate have been commonly used to study the impairment of hepatic lipid metabolism and steatosis related to NAFLD (Gomez-Lechon et al. 2007, Kanuri and Bergheim 2013, Kim et al. 2019), representing an appropriate cellular model to determine the involvement of AMPK activation in PEA effects. PEA treatment reduced lipid accumulation induced by palmitate in HepG2 cells, activating the phosphorylation of AMPK, and the expression of PPAR-α and CPT1. Notably, PEA effects were blunted by AMPK inhibition, evidencing the involvement of this enzyme in PEA-induced improvement of hepatic lipid metabolism in challenged hepatocytes These results demonstrated that, acting via AMPK pathway, PEA control multiple side of cellular metabolism, including lipid oxidation, mitochondrial function and efficiency. As mentioned before, AMPK coordinates metabolism via multiple functions (controlling ATP rates, orchestrating cellular metabolism and ensuring mitochondrial health), and the possibility to activate this kinase is considered a harmful tool to counteract NAFLD (Herzig and Shaw 2018).

In the last part of the PhD course, the intriguing possibility to impact on energy expenditure prompted the study towards the investigation of BAT, the unique organ able to perform non-shivering thermogenesis. Light microscopy of iBAT revealed a multilocular rearrangement of brown adipocytes in obese mice treated with PEA, demonstrating its capability to rescue BAT whitening induced by HFD. In the same organ, PEA treatment induced an increased positivity for UCP1 immunohistochemical staining. Moreover, PEA increased the number of sympathetic fibers, mirroring a more functional status of iBAT (Morrison and Madden 2014, Fischer et al. 2019).

As previous implied, UCP1 is the obligatory thermogenic protein by which BAT dissipates energy in form of heat and its activity decreases metabolic efficiency (Cannon and Nedergaard 2004). Although UCP1-ablated mice do not develop spontaneously obesity, they are more susceptible to high-fat feeding and prone to gain fat adiposity (von Essen et al. 2017).

In rodents and human, to enroll the thermogenic potential of BAT via UCP1 is of considerable interest to counteract the development of obesity. Under normal or obesogenic feeding conditions, we should consider the contribution of UCP1 activity to diet-induced thermogenesis (DIT), the obligatory or adaptative (facultative) process occurring in response to food intake. Paradoxically, in short-term high-fat feeding mice, body adiposity positively correlates with total UCP1 content, a physiological feature which reflects the requirement of the body to the diet-adaptative thermogenic mechanism. It means that the magnitude of the thermogenic response depends on the amount of eaten food (higher food intake leads to higher thermogenesis) (von Essen et al. 2017). However, DIT represent a homeostatic mechanism that counteracts the further development of obesity,

but the metabolic inflexibility, occurring during chronic overfeeding, failed in body adaptation to the excessive energy intake.

The experimental data obtained demonstrated that PEA treatment promoted the iBAT thermogenic adaptation to the energy gained from the diet, increasing the number of UCP1-positive cluster of brown adipocytes that perfectly matches with the recovery of the typical iBAT morphology. PEA-induced activation of iBAT was also confirmed by the mRNA expression of several thermogenic marker (UCP1, PGC1α, PRDM16, COX8B*)*.

Moreover, PEA-treated animals showed an increased gene expression of thermogenic marker of beiging (UCP1, PGC1α and PRDM16) in scWAT, also demonstrating the recruitment of beige adipocytes in the inguinal depots. The thermogenic capacity of beige cells is mainly due to the presence of mitochondria provided of UCP1. An emerging role for AMPK in the modulation of mitochondrial health has been widely recognized both in brown and in beige cells (Mottillo et al. 2016). Even in scWAT, PEA enhanced the activation of AMPK pathway, and increased the protein expression of PGC1α a master driver of mitochondrial biogenesis. Consistently our previous data evidenced PEA capability to increase AMPK activation also in adipose tissue of ovariectomized rats with mild obesity, inhibiting cytokine synthesis and M1/M2 shift depolarization reducing the activated state of macrophages (Mattace Raso et al. 2014). The increased AMPK-phosphorylation induced by PEA was determined both in hypothalamus and WAT of ovariectomized rats.

Furthermore, PEA treatment restored leptin-signaling pathway in WAT, promoting the phosphorylation of the downstream target of leptin receptor STAT3, reducing the protein expression of the inhibitory SOCS3 and, also dampening adipose leptin resistance. Beyond the well-known endocrine

function, leptin orchestrates immunometabolism, participating to the interplay between immune cell and systemic metabolism. In fact, besides the endocrine side of adipocytes secreting leptin and adiponectin, resident and circulating macrophages are responsible of adipose tissue inflammation, producing the inflammatory cytokines (TNF-α, IL-6, monocyte chemoattractant protein-1) and contributing to the development of systemic low-grade inflammation (Larabee et al. 2020). The interplay between adipocytes and macrophages is central to the development of inflammation within the tissue. In obese mice, PEA exerts its anti-inflammatory properties, significantly increasing mRNA transcription of anti-inflammatory factors (Il-10, adiponectin and PPAR-α) and decreasing inflammatory cytokines (IL-6 and TNF- α).

Based on these results, PEA can be considered a therapeutic tool to recover metabolic flexibility impaired by obesity. All these results demonstrate that in liver PEA limit metabolic alteration, counteracting lipid accumulation in liver and adipose organ, two of the main tissues involved in the control of body energy homeostasis, restoring energy balance and impacting on adipose tissue plasticity.

Overall, the study has some limitations. As above reported, in a multifactorial disease as NALFD, the contribute of the *per se* anti-inflammatory effect of PEA on metabolic improvement could not be ruled out. Indeed, it is conceivable that this effect of PEA may sustain and amplify its metabolic activity. Moreover, our experimental condition could not allow to define whether PEA itself induced brown-to-white transdifferentiation in HFD mice for several reasons. First, HFD and HFD+PEA animals were exposed to a long-term overfeeding, undergoing a deep change of fat pad, including the disappearance of beige adipocytes in inguinal adipose depot.

Cold exposure is the most physiological cue leading browning process, since mice need to increase their rate metabolism to counterbalance the increased heat lost (Nedergaard and Cannon 2014). However, this phenomenon can be also triggered by β3-adrenergic stimulation. According to a large part of literature, the ideal condition to demonstrate PEA effect on browning would be to expose the mice at cold. Low temperature exposure would allow to evidence the browning of subcutaneous adipose tissue. To overcome the limitations of *in vivo* experimental condition, the research moved toward the *in vitro* approach. To resemble the cold adaptative response, we analyzed PEA effect in mature adipocytes upon β3-adrenergic stimulation by isoproterenol, confirming the effect evidenced in *in vivo* model of obesity.
In light of these consideration, the study provides novel insight into the metabolic effects of PEA, that may be the result of multiple direct and/or indirect converging mechanisms: the improvement of mitochondrial respiratory capacity, the decrease in mitochondrial efficiency, the improvement of redox status associated to cytoprotective defenses and its well- known anti-inflammatory effect.

General conclusion

PPAR-α constitutes a regulatory crossroad among several cellular functions as metabolism, behavior, pain perception and inflammation (Bougarne et al 2018). Despite its biological importance, the pharmacological activation of PPAR-α induced by fibrates is associated with the onset of severe adverse effects in patients with dyslipidemia and reduced efficacy in clinical management of NAFLD. This relatively weak potency may be ascribed to the selective transcriptional events induced by fibrates, whose metabolic effect are unable to counteract a complex disease such as NAFLD. Indeed, NAFLD belongs to a cluster of metabolic abnormalities associated with obesity, whose metabolic complication are mainly due to the chronic pro-inflammatory status, to date known as "metaflammation".

A safe therapy for obesity and related disorders is still a pharmacological challenge, and future research is moving towards the pan or dual-PPAR (α/γ or α/δ) modulators, with a broad-spectrum pharmacological activity and a minimal risk of side effects (Friedman et al. 2018).

However, for its pleiotropic activities, the ALIAmide PEA could be considered a valuable lipid compound for the multitarget approach in the prevention and therapy of obesity-related diseases, including NAFLD. Indeed, its numerous and converging direct and indirect effects depend on a more "physiological" activation of PPAR-α and AMPK modulation by which PEA exerts metabolic functions and modulate inflammation, the pathophysiological and shared starting point for obesity, IR and related disorders. Moreover, further preclinical and clinical studies on the possible association between PEA and available metabolic drugs will be necessary.

Highlights

- In healthy individuals, metabolic flexibility describes the ability to to select metabolic fuel depending on environmental demand.
- Palmitoylethanolamide is an endogenous lipid mediator and a PPAR-a agonist.
- The onset of inflexibility is a hallmark of obesity and -related disorder.
- Liver and Adipose tissue are key organ involved in energy and immune-metabolic regulation
- Palmitoylethanolamide enhances lipid metabolism reducing hepatic mitochondrial dysfunction and promoting adipose tissue plasticity.

References

Abdulnour, J., S. Yasari, R. Rabasa-Lhoret, M. Faraj, S. Petrosino, F. Piscitelli, D. Prud' Homme and V. Di Marzo (2014). "Circulating endocannabinoids in insulin sensitive vs. insulin resistant obese postmenopausal women. A MONET group study." Obesity (Silver Spring) **22**(1): 211-216.

Aebi, H. (1984). "Catalase in vitro." Methods Enzymol **105**: 121-126.

Ahern, G. P. (2003). "Activation of TRPV1 by the satiety factor oleoylethanolamide." J Biol Chem **278**(33): 30429-30434.

Alexson, S. E. and J. Nedergaard (1988). "A novel type of short- and medium-chain acyl-CoA hydrolases in brown adipose tissue mitochondria." J Biol Chem **263**(27): 13564-13571.

Alhouayek, M. and G. G. Muccioli (2014). "Harnessing the anti-inflammatory potential of palmitoylethanolamide." Drug Discov Today **19**(10): 1632-1639.

Aloe, L., A. Leon and R. Levi-Montalcini (1993). "A proposed autacoid mechanism controlling mastocyte behaviour." Agents Actions **39 Spec No**: C145-147.

Andresen, S. R., J. Bing, R. M. Hansen, F. Biering-Sorensen, I. L. Johannesen, E. M. Hagen, A. S. Rice, J. F. Nielsen, F. W. Bach and N. B. Finnerup (2016). "Ultramicronized palmitoylethanolamide in spinal cord injury neuropathic pain: a randomized, double-blind, placebo-controlled trial." Pain **157**(9): 2097-2103.

Arch, J. R. (2011). "Challenges in beta(3)-Adrenoceptor Agonist Drug Development." Ther Adv Endocrinol Metab **2**(2): 59-64.

Astrup, A., S. Rossner, L. Van Gaal, A. Rissanen, L. Niskanen, M. Al Hakim, J. Madsen, M. F. Rasmussen, M. E. Lean and N. N. S. Group (2009). "Effects of liraglutide in the treatment of obesity: a randomised, double-blind, placebo-controlled study." Lancet **374**(9701): 1606-1616.

Avagliano, C., R. Russo, C. De Caro, C. Cristiano, G. La Rana, G. Piegari, O. Paciello, R. Citraro, E. Russo, G. De Sarro, R. Meli, G. Mattace Raso and A. Calignano (2016). "Palmitoylethanolamide protects mice against 6-OHDA-induced neurotoxicity and endoplasmic reticulum stress: In vivo and in vitro evidence." Pharmacol Res **113**(Pt A): 276-289.

Awazawa, M., K. Ueki, K. Inabe, T. Yamauchi, K. Kaneko, Y. Okazaki, N. Bardeesy, S. Ohnishi, R. Nagai and T. Kadowaki (2009). "Adiponectin suppresses hepatic SREBP1c expression in an

AdipoR1/LKB1/AMPK dependent pathway." Biochem Biophys Res Commun **382**(1): 51-56.
Bachur, N. R., K. Masek, K. L. Melmon and S. Udenfriend (1965). "Fatty Acid Amides of Ethanolamine in Mammalian Tissues." J Biol Chem **240**: 1019-1024.
Barbera, M. J., A. Schluter, N. Pedraza, R. Iglesias, F. Villarroya and M. Giralt (2001). "Peroxisome proliferator-activated receptor alpha activates transcription of the brown fat uncoupling protein-1 gene. A link between regulation of the thermogenic and lipid oxidation pathways in the brown fat cell." J Biol Chem **276**(2): 1486-1493.
Battaglia, G. M., D. Zheng, R. C. Hickner and J. A. Houmard (2012). "Effect of exercise training on metabolic flexibility in response to a high-fat diet in obese individuals." Am J Physiol Endocrinol Metab **303**(12): E1440-1445.
Begriche, K., J. Massart, M. A. Robin, F. Bonnet and B. Fromenty (2013). "Mitochondrial adaptations and dysfunctions in nonalcoholic fatty liver disease." Hepatology **58**(4): 1497-1507.
Beiroa, D., M. Imbernon, R. Gallego, A. Senra, D. Herranz, F. Villarroya, M. Serrano, J. Ferno, J. Salvador, J. Escalada, C. Dieguez, M. Lopez, G. Fruhbeck and R. Nogueiras (2014). "GLP-1 agonism stimulates brown adipose tissue thermogenesis and browning through hypothalamic AMPK." Diabetes **63**(10): 3346-3358.
Bensinger, S. J. and P. Tontonoz (2008). "Integration of metabolism and inflammation by lipid-activated nuclear receptors." Nature **454**(7203): 470-477.
Bergamo, P., F. Maurano and M. Rossi (2007). "Phase 2 enzyme induction by conjugated linoleic acid improves lupus-associated oxidative stress." Free Radic Biol Med **43**(1): 71-79.
Borrelli, F., B. Romano, S. Petrosino, E. Pagano, R. Capasso, D. Coppola, G. Battista, P. Orlando, V. Di Marzo and A. A. Izzo (2015). "Palmitoylethanolamide, a naturally occurring lipid, is an orally effective intestinal anti-inflammatory agent." Br J Pharmacol **172**(1): 142-158.
Bottemanne, P., G. G. Muccioli and M. Alhouayek (2018). "N-acylethanolamine hydrolyzing acid amidase inhibition: tools and potential therapeutic opportunities." Drug Discov Today **23**(8): 1520-1529.
Bougarne, N., B. Weyers, S. J. Desmet, J. Deckers, D. W. Ray, B. Staels and K. De Bosscher (2018). "Molecular Actions of PPARalpha in Lipid Metabolism and Inflammation." Endocr Rev **39**(5): 760-802.
Bouillaud, F., M. C. Alves-Guerra and D. Ricquier (2016). "UCPs, at the interface between bioenergetics and metabolism." Biochim Biophys Acta **1863**(10): 2443-2456.

Calignano, A., G. La Rana, A. Giuffrida and D. Piomelli (1998). "Control of pain initiation by endogenous cannabinoids." Nature **394**(6690): 277-281.
Calignano, A., G. La Rana and D. Piomelli (2001). "Antinociceptive activity of the endogenous fatty acid amide, palmitylethanolamide." Eur J Pharmacol **419**(2-3): 191-198.
Camell, C. D., J. Sander, O. Spadaro, A. Lee, K. Y. Nguyen, A. Wing, E. L. Goldberg, Y. H. Youm, C. W. Brown, J. Elsworth, M. S. Rodeheffer, J. L. Schultze and V. D. Dixit (2017). "Inflammasome-driven catecholamine catabolism in macrophages blunts lipolysis during ageing." Nature **550**(7674): 119-123.
Cannon, B. and J. Nedergaard (2004). "Brown adipose tissue: function and physiological significance." Physiol Rev **84**(1): 277-359.
Cao, J., D. L. Dai, L. Yao, H. H. Yu, B. Ning, Q. Zhang, J. Chen, W. H. Cheng, W. Shen and Z. X. Yang (2012). "Saturated fatty acid induction of endoplasmic reticulum stress and apoptosis in human liver cells via the PERK/ATF4/CHOP signaling pathway." Mol Cell Biochem **364**(1-2): 115-129.
Capasso, R., A. A. Izzo, F. Fezza, A. Pinto, F. Capasso, N. Mascolo and V. Di Marzo (2001). "Inhibitory effect of palmitoylethanolamide on gastrointestinal motility in mice." Br J Pharmacol **134**(5): 945-950.
Caputo, T., F. Gilardi and B. Desvergne (2017). "From chronic overnutrition to metaflammation and insulin resistance: adipose tissue and liver contributions." FEBS Lett **591**(19): 3061-3088.
Carta, G., E. Murru, S. Banni and C. Manca (2017). "Palmitic Acid: Physiological Role, Metabolism and Nutritional Implications." Front Physiol **8**: 902.
Cavaliere, G., G. Trinchese, P. Bergamo, C. De Filippo, G. Mattace Raso, G. Gifuni, R. Putti, B. H. Moni, R. B. Canani, R. Meli and M. P. Mollica (2016). "Polyunsaturated Fatty Acids Attenuate Diet Induced Obesity and Insulin Resistance, Modulating Mitochondrial Respiratory Uncoupling in Rat Skeletal Muscle." PLoS One **11**(2): e0149033.
Cerrato, S., P. Brazis, M. F. Della Valle, A. Miolo, S. Petrosino, V. Di Marzo and A. Puigdemont (2012). "Effects of palmitoylethanolamide on the cutaneous allergic inflammatory response in Ascaris hypersensitive Beagle dogs." Vet J **191**(3): 377-382.
Cerrato, S., P. Brazis, M. F. della Valle, A. Miolo and A. Puigdemont (2010). "Effects of palmitoylethanolamide on immunologically induced histamine, PGD2 and TNFalpha release from canine skin mast cells." Vet Immunol Immunopathol **133**(1): 9-15.

Chang, H. C. and L. Guarente (2014). "SIRT1 and other sirtuins in metabolism." Trends Endocrinol Metab **25**(3): 138-145.
Chen, L., L. Li, J. Chen, L. Li, Z. Zheng, J. Ren and Y. Qiu (2015). "Oleoylethanolamide, an endogenous PPAR-alpha ligand, attenuates liver fibrosis targeting hepatic stellate cells." Oncotarget **6**(40): 42530-42540.
Chouchani, E. T., L. Kazak and B. M. Spiegelman (2019). "New Advances in Adaptive Thermogenesis: UCP1 and Beyond." Cell Metab **29**(1): 27-37.
Cinti, S. (2002). "Adipocyte differentiation and transdifferentiation: plasticity of the adipose organ." J Endocrinol Invest **25**(10): 823-835.
Cinti, S. (2012). "The adipose organ at a glance." Dis Model Mech **5**(5): 588-594.
Cinti, S. (2018). "Adipose Organ Development and Remodeling." Compr Physiol **8**(4): 1357-1431.
Cipriani, S., A. Mencarelli, G. Palladino and S. Fiorucci (2010). "FXR activation reverses insulin resistance and lipid abnormalities and protects against liver steatosis in Zucker (fa/fa) obese rats." J Lipid Res **51**(4): 771-784.
Cravatt, B. F., D. K. Giang, S. P. Mayfield, D. L. Boger, R. A. Lerner and N. B. Gilula (1996). "Molecular characterization of an enzyme that degrades neuromodulatory fatty-acid amides." Nature **384**(6604): 83-87.
Cruccu, G., G. D. Stefano, P. Marchettini and A. Truini (2019). "Micronized Palmitoylethanolamide: A Post Hoc Analysis of a Controlled Study in Patients with Low Back Pain - Sciatica." CNS Neurol Disord Drug Targets **18**(6): 491-495.
Cypess, A. M., S. Lehman, G. Williams, I. Tal, D. Rodman, A. B. Goldfine, F. C. Kuo, E. L. Palmer, Y. H. Tseng, A. Doria, G. M. Kolodny and C. R. Kahn (2009). "Identification and importance of brown adipose tissue in adult humans." N Engl J Med **360**(15): 1509-1517.
D'Agostino, G., G. La Rana, R. Russo, O. Sasso, A. Iacono, E. Esposito, G. Mattace Raso, S. Cuzzocrea, J. Loverme, D. Piomelli, R. Meli and A. Calignano (2009). "Central administration of palmitoylethanolamide reduces hyperalgesia in mice via inhibition of NF-kappaB nuclear signalling in dorsal root ganglia." Eur J Pharmacol **613**(1-3): 54-59.
Day, E. A., R. J. Ford and G. R. Steinberg (2017). "AMPK as a Therapeutic Target for Treating Metabolic Diseases." Trends Endocrinol Metab **28**(8): 545-560.
de Ligt, M., S. Timmers and P. Schrauwen (2015). "Resveratrol and obesity: Can resveratrol relieve metabolic disturbances?" Biochim Biophys Acta **1852**(6): 1137-1144.

de Mello, A. H., A. B. Costa, J. D. G. Engel and G. T. Rezin (2017). "Mitochondrial dysfunction in obesity." Life sciences.
De Petrocellis, L., C. J. Chu, A. S. Moriello, J. C. Kellner, J. M. Walker and V. Di Marzo (2004). "Actions of two naturally occurring saturated N-acyldopamines on transient receptor potential vanilloid 1 (TRPV1) channels." Br J Pharmacol **143**(2): 251-256.
De Petrocellis, L., J. B. Davis and V. Di Marzo (2001). "Palmitoylethanolamide enhances anandamide stimulation of human vanilloid VR1 receptors." FEBS Lett **506**(3): 253-256.
Desvergne, B. and W. Wahli (1999). "Peroxisome proliferator-activated receptors: nuclear control of metabolism." Endocr Rev **20**(5): 649-688.
Devane, W. A., L. Hanus, A. Breuer, R. G. Pertwee, L. A. Stevenson, G. Griffin, D. Gibson, A. Mandelbaum, A. Etinger and R. Mechoulam (1992). "Isolation and structure of a brain constituent that binds to the cannabinoid receptor." Science **258**(5090): 1946-1949.
Di Marzo, V., S. K. Goparaju, L. Wang, J. Liu, S. Batkai, Z. Jarai, F. Fezza, G. I. Miura, R. D. Palmiter, T. Sugiura and G. Kunos (2001). "Leptin-regulated endocannabinoids are involved in maintaining food intake." Nature **410**(6830): 822-825.
Diano, S. and T. L. Horvath (2012). "Mitochondrial uncoupling protein 2 (UCP2) in glucose and lipid metabolism." Trends in Molecular Medicine **18**(1): 52-58.
Divakaruni, A. S., A. Paradyse, D. A. Ferrick, A. N. Murphy and M. Jastroch (2014). Analysis and interpretation of microplate-based oxygen consumption and pH data. Methods in enzymology, Elsevier. **547:** 309-354.
Dominguez, J. F., L. Guo, M. A. Carrasco Molnar, A. Ballester Escobedo, T. Dunphy, T. D. Lund and J. E. Turman, Jr. (2009). "Novel indirect calorimetry technology to analyze metabolism in individual neonatal rodent pups." PLoS One **4**(8): e6790.
Endocannabinoid Research, G., D. De Filippis, A. D'Amico, M. Cipriano, S. Petrosino, P. Orlando, V. Di Marzo and T. Iuvone (2010). "Levels of endocannabinoids and palmitoylethanolamide and their pharmacological manipulation in chronic granulomatous inflammation in rats." Pharmacol Res **61**(4): 321-328.
Esposito, G., E. Capoccia, F. Turco, I. Palumbo, J. Lu, A. Steardo, R. Cuomo, G. Sarnelli and L. Steardo (2014). "Palmitoylethanolamide improves colon inflammation through an enteric glia/toll like receptor 4-dependent PPAR-alpha activation." Gut **63**(8): 1300-1312.
Facci, L., R. Dal Toso, S. Romanello, A. Buriani, S. D. Skaper and A. Leon (1995). "Mast cells express a peripheral cannabinoid receptor with

differential sensitivity to anandamide and palmitoylethanolamide." Proc Natl Acad Sci U S A **92**(8): 3376-3380.
Fanelli, F., M. Mezzullo, A. Repaci, I. Belluomo, D. Ibarra Gasparini, G. Di Dalmazi, M. Mastroroberto, V. Vicennati, A. Gambineri, A. M. Morselli-Labate, R. Pasquali and U. Pagotto (2018). "Profiling plasma N-Acylethanolamine levels and their ratios as a biomarker of obesity and dysmetabolism." Mol Metab **14**: 82-94.
Ferrante, M. C., P. Amero, A. Santoro, A. Monnolo, R. Simeoli, F. Di Guida, G. Mattace Raso and R. Meli (2014). "Polychlorinated biphenyls (PCB 101, PCB 153 and PCB 180) alter leptin signaling and lipid metabolism in differentiated 3T3-L1 adipocytes." Toxicol Appl Pharmacol **279**(3): 401-408.
Fischer, A. W., C. Schlein, B. Cannon, J. Heeren and J. Nedergaard (2019). "Intact innervation is essential for diet-induced recruitment of brown adipose tissue." Am J Physiol Endocrinol Metab **316**(3): E487-E503.
Flohe, L. and F. Otting (1984). "Superoxide dismutase assays." Methods Enzymol **105**: 93-104.
Friedman, S. L., B. A. Neuschwander-Tetri, M. Rinella and A. J. Sanyal (2018). "Mechanisms of NAFLD development and therapeutic strategies." Nat Med **24**(7): 908-922.
Fu, J., S. Gaetani, F. Oveisi, J. Lo Verme, A. Serrano, F. Rodriguez De Fonseca, A. Rosengarth, H. Luecke, B. Di Giacomo, G. Tarzia and D. Piomelli (2003). "Oleylethanolamide regulates feeding and body weight through activation of the nuclear receptor PPAR-alpha." Nature **425**(6953): 90-93.
Gabrielsson, L., S. Mattsson and C. J. Fowler (2016). "Palmitoylethanolamide for the treatment of pain: pharmacokinetics, safety and efficacy." Br J Clin Pharmacol **82**(4): 932-942.
Ghorbani, M., T. H. Claus and J. Himms-Hagen (1997). "Hypertrophy of brown adipocytes in brown and white adipose tissues and reversal of diet-induced obesity in rats treated with a beta3-adrenoceptor agonist." Biochem Pharmacol **54**(1): 121-131.
Giammusso, B., R. Di Mauro and R. Bernardini (2017). "The efficacy of an association of palmitoylethanolamide and alpha-lipoic acid in patients with chronic prostatitis/chronic pelvic pain syndrome: A randomized clinical trial." Arch Ital Urol Androl **89**(1): 17-21.
Giordano, A., A. Frontini and S. Cinti (2016). "Convertible visceral fat as a therapeutic target to curb obesity." Nat Rev Drug Discov **15**(6): 405-424.
Godlewski, G., L. Offertaler, J. A. Wagner and G. Kunos (2009). "Receptors for acylethanolamides-GPR55 and GPR119." Prostaglandins Other Lipid Mediat **89**(3-4): 105-111.

Gomes, L. C. and L. Scorrano (2011). "Mitochondrial elongation during autophagy: a stereotypical response to survive in difficult times." Autophagy **7**(10): 1251-1253.
Gomez-Lechon, M. J., M. T. Donato, A. Martinez-Romero, N. Jimenez, J. V. Castell and J. E. O'Connor (2007). "A human hepatocellular in vitro model to investigate steatosis." Chem Biol Interact **165**(2): 106-116.
Gouveia-Figueira, S. and M. L. Nording (2014). "Development and validation of a sensitive UPLC-ESI-MS/MS method for the simultaneous quantification of 15 endocannabinoids and related compounds in milk and other biofluids." Anal Chem **86**(2): 1186-1195.
Guzmán, M., J. L. Verme, J. Fu, F. Oveisi, C. Blázquez and D. Piomelli (2004). "Oleoylethanolamide stimulates lipolysis by activating the nuclear receptor peroxisome proliferator-activated receptor α (PPAR-α)." Journal of biological chemistry **279**(27): 27849-27854.
Handy, J. A., P. P. Fu, P. Kumar, J. E. Mells, S. Sharma, N. K. Saxena and F. A. Anania (2011). "Adiponectin inhibits leptin signalling via multiple mechanisms to exert protective effects against hepatic fibrosis." Biochem J **440**(3): 385-395.
Hao, L., S. Scott, M. Abbasi, Y. Zu, M. S. H. Khan, Y. Yang, D. Wu, L. Zhao and S. Wang (2019). "Beneficial Metabolic Effects of Mirabegron In Vitro and in High-Fat Diet-Induced Obese Mice." J Pharmacol Exp Ther **369**(3): 419-427.
Harms, M. and P. Seale (2013). "Brown and beige fat: development, function and therapeutic potential." Nat Med **19**(10): 1252-1263.
Harrison, S. A., M. E. Rinella, M. F. Abdelmalek, J. F. Trotter, A. H. Paredes, H. L. Arnold, M. Kugelmas, M. R. Bashir, M. J. Jaros, L. Ling, S. J. Rossi, A. M. DePaoli and R. Loomba (2018). "NGM282 for treatment of non-alcoholic steatohepatitis: a multicentre, randomised, double-blind, placebo-controlled, phase 2 trial." Lancet **391**(10126): 1174-1185.
Hartree, E. F. (1972). "Determination of protein: a modification of the Lowry method that gives a linear photometric response." Anal Biochem **48**(2): 422-427.
Hausladen, A. and I. Fridovich (1996). "Measuring nitric oxide and superoxide: rate constants for aconitase reactivity." Methods Enzymol **269**: 37-41.
Herzig, S. and R. J. Shaw (2018). "AMPK: guardian of metabolism and mitochondrial homeostasis." Nat Rev Mol Cell Biol **19**(2): 121-135.
Ho, W. S., D. A. Barrett and M. D. Randall (2008). "'Entourage' effects of N-palmitoylethanolamide and N-oleoylethanolamide on vasorelaxation to anandamide occur through TRPV1 receptors." Br J Pharmacol **155**(6): 837-846.

Hondares, E., M. Rosell, J. Diaz-Delfin, Y. Olmos, M. Monsalve, R. Iglesias, F. Villarroya and M. Giralt (2011). "Peroxisome proliferator-activated receptor alpha (PPARalpha) induces PPARgamma coactivator 1alpha (PGC-1alpha) gene expression and contributes to thermogenic activation of brown fat: involvement of PRDM16." J Biol Chem **286**(50): 43112-43122.

Inagaki, T., P. Dutchak, G. Zhao, X. Ding, L. Gautron, V. Parameswara, Y. Li, R. Goetz, M. Mohammadi, V. Esser, J. K. Elmquist, R. D. Gerard, S. C. Burgess, R. E. Hammer, D. J. Mangelsdorf and S. A. Kliewer (2007). "Endocrine regulation of the fasting response by PPARalpha-mediated induction of fibroblast growth factor 21." Cell Metab **5**(6): 415-425.

Izzo, A. A., R. Capasso, G. Aviello, F. Borrelli, B. Romano, F. Piscitelli, L. Gallo, F. Capasso, P. Orlando and V. Di Marzo (2012). "Inhibitory effect of cannabichromene, a major non-psychotropic cannabinoid extracted from Cannabis sativa, on inflammation-induced hypermotility in mice." Br J Pharmacol **166**(4): 1444-1460.

Izzo, A. A., F. Piscitelli, R. Capasso, P. Marini, L. Cristino, S. Petrosino and V. Di Marzo (2010). "Basal and fasting/refeeding-regulated tissue levels of endogenous PPAR-alpha ligands in Zucker rats." Obesity (Silver Spring) **18**(1): 55-62.

Jhaveri, M. D., D. Richardson, I. Robinson, M. J. Garle, A. Patel, Y. Sun, D. R. Sagar, A. J. Bennett, S. P. Alexander, D. A. Kendall, D. A. Barrett and V. Chapman (2008). "Inhibition of fatty acid amide hydrolase and cyclooxygenase-2 increases levels of endocannabinoid related molecules and produces analgesia via peroxisome proliferator-activated receptor-alpha in a model of inflammatory pain." Neuropharmacology **55**(1): 85-93.

Jin, X., Z. Xiang, Y. P. Chen, K. F. Ma, Y. F. Ye and Y. M. Li (2013). "Uncoupling protein and nonalcoholic fatty liver disease." Chin Med J (Engl) **126**(16): 3151-3155.

Kanuri, G. and I. Bergheim (2013). "In vitro and in vivo models of non-alcoholic fatty liver disease (NAFLD)." Int J Mol Sci **14**(6): 11963-11980.

Khan, R. S., F. Bril, K. Cusi and P. N. Newsome (2019). "Modulation of Insulin Resistance in Nonalcoholic Fatty Liver Disease." Hepatology **70**(2): 711-724.

Kim, K., G. D. Bae, M. Lee, E. Y. Park, D. J. Baek, C. Y. Kim, H. S. Jun and Y. S. Oh (2019). "Allomyrina dichotoma Larva Extract Ameliorates the Hepatic Insulin Resistance of High-Fat Diet-Induced Diabetic Mice." Nutrients **11**(7).

Kim, Y., Y. Chang, Y. K. Cho, J. Ahn, H. Shin and S. Ryu (2019). "Obesity and Weight Gain Are Associated With Progression of Fibrosis in Patients With Nonalcoholic Fatty Liver Disease." Clin Gastroenterol Hepatol **17**(3): 543-550 e542.
Kleiner, D. E., E. M. Brunt, M. Van Natta, C. Behling, M. J. Contos, O. W. Cummings, L. D. Ferrell, Y. C. Liu, M. S. Torbenson, A. Unalp-Arida, M. Yeh, A. J. McCullough, A. J. Sanyal and N. Nonalcoholic Steatohepatitis Clinical Research (2005). "Design and validation of a histological scoring system for nonalcoholic fatty liver disease." Hepatology **41**(6): 1313-1321.
Koliaki, C., J. Szendroedi, K. Kaul, T. Jelenik, P. Nowotny, F. Jankowiak, C. Herder, M. Carstensen, M. Krausch, W. T. Knoefel, M. Schlensak and M. Roden (2015). "Adaptation of hepatic mitochondrial function in humans with non-alcoholic fatty liver is lost in steatohepatitis." Cell Metab **21**(5): 739-746.
Konrad, D. and S. Wueest (2014). "The gut-adipose-liver axis in the metabolic syndrome." Physiology (Bethesda) **29**(5): 304-313.
Kusminski, C. M., P. E. Bickel and P. E. Scherer (2016). "Targeting adipose tissue in the treatment of obesity-associated diabetes." Nat Rev Drug Discov **15**(9): 639-660.
Laleh, P., K. Yaser, B. Abolfazl, A. Shahriar, A. J. Mohammad, F. Nazila and O. Alireza (2018). "Oleoylethanolamide increases the expression of PPAR-Alpha and reduces appetite and body weight in obese people: A clinical trial." Appetite **128**: 44-49.
Lama, A., C. Pirozzi, M. P. Mollica, G. Trinchese, F. Di Guida, G. Cavaliere, A. Calignano, G. Mattace Raso, R. Berni Canani and R. Meli (2017). "Polyphenol-rich virgin olive oil reduces insulin resistance and liver inflammation and improves mitochondrial dysfunction in high-fat diet fed rats." Mol Nutr Food Res **61**(3).
Larabee, C. M., O. C. Neely and A. I. Domingos (2020). "Obesity: a neuroimmunometabolic perspective." Nat Rev Endocrinol **16**(1): 30-43.
Lauffer, L. M., R. Iakoubov and P. L. Brubaker (2009). "GPR119 is essential for oleoylethanolamide-induced glucagon-like peptide-1 secretion from the intestinal enteroendocrine L-cell." Diabetes **58**(5): 1058-1066.
Lee, Y., X. Yu, F. Gonzales, D. J. Mangelsdorf, M. Y. Wang, C. Richardson, L. A. Witters and R. H. Unger (2002). "PPAR alpha is necessary for the lipopenic action of hyperleptinemia on white adipose and liver tissue." Proc Natl Acad Sci U S A **99**(18): 11848-11853.
Lee, Y. K., J. H. Sohn, J. S. Han, Y. J. Park, Y. G. Jeon, Y. Ji, K. T. Dalen, C. Sztalryd, A. R. Kimmel and J. B. Kim (2018). "Perilipin 3

Deficiency Stimulates Thermogenic Beige Adipocytes Through PPARalpha Activation." Diabetes **67**(5): 791-804.
Li, L., D. W. Liu, H. Y. Yan, Z. Y. Wang, S. H. Zhao and B. Wang (2016). "Obesity is an independent risk factor for non-alcoholic fatty liver disease: evidence from a meta-analysis of 21 cohort studies." Obes Rev **17**(6): 510-519.
Lihn, A. S., S. B. Pedersen, S. Lund and B. Richelsen (2008). "The anti-diabetic AMPK activator AICAR reduces IL-6 and IL-8 in human adipose tissue and skeletal muscle cells." Mol Cell Endocrinol **292**(1-2): 36-41.
Lo Verme, J., J. Fu, G. Astarita, G. La Rana, R. Russo, A. Calignano and D. Piomelli (2005). "The nuclear receptor peroxisome proliferator-activated receptor-alpha mediates the anti-inflammatory actions of palmitoylethanolamide." Mol Pharmacol **67**(1): 15-19.
Locci, A. and G. Pinna (2019). "Stimulation of Peroxisome Proliferator-Activated Receptor-alpha by N-Palmitoylethanolamine Engages Allopregnanolone Biosynthesis to Modulate Emotional Behavior." Biol Psychiatry **85**(12): 1036-1045.
Loh, R. K. C., M. F. Formosa, A. La Gerche, A. T. Reutens, B. A. Kingwell and A. L. Carey (2019). "Acute metabolic and cardiovascular effects of mirabegron in healthy individuals." Diabetes Obes Metab **21**(2): 276-284.
Loncar, D. (1991). "Convertible adipose tissue in mice." Cell Tissue Res **266**(1): 149-161.
Long, D. A. and A. J. Martin (1956). "Factor in arachis oil depressing sensitivity to tuberculin in B.C.G.-infected guineapigs." Lancet **270**(6921): 464-466.
Long, Y. C. and J. R. Zierath (2006). "AMP-activated protein kinase signaling in metabolic regulation." J Clin Invest **116**(7): 1776-1783.
Lopez-Lluch, G. (2017). "Mitochondrial activity and dynamics changes regarding metabolism in ageing and obesity." Mech Ageing Dev **162**: 108-121.
Mailloux, R. J. and M. E. Harper (2011). "Uncoupling proteins and the control of mitochondrial reactive oxygen species production." Free Radic Biol Med **51**(6): 1106-1115.
Mansouri, A., C. H. Gattolliat and T. Asselah (2018). "Mitochondrial Dysfunction and Signaling in Chronic Liver Diseases." Gastroenterology **155**(3): 629-647.
Marcucci, M., F. Germini, A. Coerezza, L. Andreinetti, L. Bellintani, A. Nobili, P. D. Rossi and D. Mari (2016). "Efficacy of ultra-micronized palmitoylethanolamide (um-PEA) in geriatric patients with chronic pain: study protocol for a series of N-of-1 randomized trials." Trials **17**: 369.

Mattace Raso, G., R. Russo, A. Calignano and R. Meli (2014). "Palmitoylethanolamide in CNS health and disease." Pharmacol Res **86**: 32-41.
Mattace Raso, G., A. Santoro, R. Russo, R. Simeoli, O. Paciello, C. Di Carlo, S. Diano, A. Calignano and R. Meli (2014). "Palmitoylethanolamide prevents metabolic alterations and restores leptin sensitivity in ovariectomized rats." Endocrinology **155**(4): 1291-1301.
Mazzari, S., R. Canella, L. Petrelli, G. Marcolongo and A. Leon (1996). "N-(2-hydroxyethyl)hexadecanamide is orally active in reducing edema formation and inflammatory hyperalgesia by down-modulating mast cell activation." Eur J Pharmacol **300**(3): 227-236.
Mechoulam, R., S. Ben-Shabat, L. Hanus, M. Ligumsky, N. Kaminski and A. Schatz (1995). Identification of an endogenous 2-monoglyceride, Present.
Meli, R., G. Mattace Raso and A. Calignano (2014). "Role of innate immune response in non-alcoholic Fatty liver disease: metabolic complications and therapeutic tools." Front Immunol **5**: 177.
Minokoshi, Y., Y. B. Kim, O. D. Peroni, L. G. Fryer, C. Muller, D. Carling and B. B. Kahn (2002). "Leptin stimulates fatty-acid oxidation by activating AMP-activated protein kinase." Nature **415**(6869): 339-343.
Moir, L., L. Bentley and R. D. Cox (2016). "Comprehensive Energy Balance Measurements in Mice." Curr Protoc Mouse Biol **6**(3): 211-222.
Moller, D. E. (2000). "Potential role of TNF-alpha in the pathogenesis of insulin resistance and type 2 diabetes." Trends Endocrinol Metab **11**(6): 212-217.
Mollica, M. P., G. Mattace Raso, G. Cavaliere, G. Trinchese, C. De Filippo, S. Aceto, M. Prisco, C. Pirozzi, F. Di Guida, A. Lama, M. Crispino, D. Tronino, P. Di Vaio, R. Berni Canani, A. Calignano and R. Meli (2017). "Butyrate Regulates Liver Mitochondrial Function, Efficiency, and Dynamics in Insulin-Resistant Obese Mice." Diabetes **66**(5): 1405-1418.
Montagner, A., A. Polizzi, E. Fouche, S. Ducheix, Y. Lippi, F. Lasserre, V. Barquissau, M. Regnier, C. Lukowicz, F. Benhamed, A. Iroz, J. Bertrand-Michel, T. Al Saati, P. Cano, L. Mselli-Lakhal, G. Mithieux, F. Rajas, S. Lagarrigue, T. Pineau, N. Loiseau, C. Postic, D. Langin, W. Wahli and H. Guillou (2016). "Liver PPARalpha is crucial for whole-body fatty acid homeostasis and is protective against NAFLD." Gut **65**(7): 1202-1214.
Morino, K., K. F. Petersen and G. I. Shulman (2006). "Molecular mechanisms of insulin resistance in humans and their potential links with mitochondrial dysfunction." Diabetes **55 Suppl 2**: S9-S15.

Morrison, S. F. and C. J. Madden (2014). "Central nervous system regulation of brown adipose tissue." Compr Physiol **4**(4): 1677-1713.
Mottillo, E. P., E. M. Desjardins, J. D. Crane, B. K. Smith, A. E. Green, S. Ducommun, T. I. Henriksen, I. A. Rebalka, A. Razi, K. Sakamoto, C. Scheele, B. E. Kemp, T. J. Hawke, J. Ortega, J. G. Granneman and G. R. Steinberg (2016). "Lack of Adipocyte AMPK Exacerbates Insulin Resistance and Hepatic Steatosis through Brown and Beige Adipose Tissue Function." Cell Metab **24**(1): 118-129.
Mudaliar, S., R. R. Henry, A. J. Sanyal, L. Morrow, H. U. Marschall, M. Kipnes, L. Adorini, C. I. Sciacca, P. Clopton, E. Castelloe, P. Dillon, M. Pruzanski and D. Shapiro (2013). "Efficacy and safety of the farnesoid X receptor agonist obeticholic acid in patients with type 2 diabetes and nonalcoholic fatty liver disease." Gastroenterology **145**(3): 574-582 e571.
Nedergaard, J. and B. Cannon (2014). "The browning of white adipose tissue: some burning issues." Cell Metab **20**(3): 396-407.
Nedergaard, J., B. Cannon and O. Lindberg (1977). "Microcalorimetry of isolated mammalian cells." Nature **267**(5611): 518-520.
Nielsen, M. J., G. Petersen, A. Astrup and H. S. Hansen (2004). "Food intake is inhibited by oral oleoylethanolamide." J Lipid Res **45**(6): 1027-1029.
Nies, V. J., G. Sancar, W. Liu, T. van Zutphen, D. Struik, R. T. Yu, A. R. Atkins, R. M. Evans, J. W. Jonker and M. R. Downes (2015). "Fibroblast Growth Factor Signaling in Metabolic Regulation." Front Endocrinol (Lausanne) **6**: 193.
Obre, E. and R. Rossignol (2015). "Emerging concepts in bioenergetics and cancer research: metabolic flexibility, coupling, symbiosis, switch, oxidative tumors, metabolic remodeling, signaling and bioenergetic therapy." Int J Biochem Cell Biol **59**: 167-181.
Oriente, F., S. Cabaro, A. Liotti, M. Longo, L. Parrillo, T. B. Pagano, G. A. Raciti, D. Penkov, O. Paciello, C. Miele, P. Formisano, F. Blasi and F. Beguinot (2013). "PREP1 deficiency downregulates hepatic lipogenesis and attenuates steatohepatitis in mice." Diabetologia **56**(12): 2713-2722.
Paradies, G., V. Paradies, F. M. Ruggiero and G. Petrosillo (2014). "Oxidative stress, cardiolipin and mitochondrial dysfunction in nonalcoholic fatty liver disease." World J Gastroenterol **20**(39): 14205-14218.
Pawlak, M., P. Lefebvre and B. Staels (2015). "Molecular mechanism of PPARalpha action and its impact on lipid metabolism, inflammation and fibrosis in non-alcoholic fatty liver disease." J Hepatol **62**(3): 720-733.

Pelleymounter, M. A., M. J. Cullen, M. B. Baker, R. Hecht, D. Winters, T. Boone and F. Collins (1995). "Effects of the obese gene product on body weight regulation in ob/ob mice." Science **269**(5223): 540-543.
Pellicciari, R., S. Fiorucci, E. Camaioni, C. Clerici, G. Costantino, P. R. Maloney, A. Morelli, D. J. Parks and T. M. Willson (2002). "6alpha-ethyl-chenodeoxycholic acid (6-ECDCA), a potent and selective FXR agonist endowed with anticholestatic activity." J Med Chem **45**(17): 3569-3572.
Petrosino, S., M. Cordaro, R. Verde, A. Schiano Moriello, G. Marcolongo, C. Schievano, R. Siracusa, F. Piscitelli, A. F. Peritore, R. Crupi, D. Impellizzeri, E. Esposito, S. Cuzzocrea and V. Di Marzo (2018). "Oral Ultramicronized Palmitoylethanolamide: Plasma and Tissue Levels and Spinal Anti-hyperalgesic Effect." Front Pharmacol **9**: 249.
Petrosino, S. and V. Di Marzo (2017). "The pharmacology of palmitoylethanolamide and first data on the therapeutic efficacy of some of its new formulations." Br J Pharmacol **174**(11): 1349-1365.
Petrosino, S., A. Schiano Moriello, S. Cerrato, M. Fusco, A. Puigdemont, L. De Petrocellis and V. Di Marzo (2016). "The anti-inflammatory mediator palmitoylethanolamide enhances the levels of 2-arachidonoyl-glycerol and potentiates its actions at TRPV1 cation channels." Br J Pharmacol **173**(7): 1154-1162.
Piscitelli, F., G. Carta, T. Bisogno, E. Murru, L. Cordeddu, K. Berge, S. Tandy, J. S. Cohn, M. Griinari and S. Banni (2011). "Effect of dietary krill oil supplementation on the endocannabinoidome of metabolically relevant tissues from high-fat-fed mice." Nutrition & metabolism **8**(1): 51.
Polyzos, S. A., J. Kountouras and C. S. Mantzoros (2015). "Leptin in nonalcoholic fatty liver disease: a narrative review." Metabolism **64**(1): 60-78.
Polyzos, S. A., J. Kountouras and C. S. Mantzoros (2019). "Obesity and nonalcoholic fatty liver disease: From pathophysiology to therapeutics." Metabolism **92**: 82-97.
Poulos, S. P., M. V. Dodson, M. F. Culver and G. J. Hausman (2016). "The increasingly complex regulation of adipocyte differentiation." Exp Biol Med (Maywood) **241**(5): 449-456.
Puigserver, P. and B. M. Spiegelman (2003). "Peroxisome proliferator-activated receptor-gamma coactivator 1 alpha (PGC-1 alpha): transcriptional coactivator and metabolic regulator." Endocr Rev **24**(1): 78-90.
Qi, Y., N. Takahashi, S. M. Hileman, H. R. Patel, A. H. Berg, U. B. Pajvani, P. E. Scherer and R. S. Ahima (2004). "Adiponectin acts in the brain to decrease body weight." Nat Med **10**(5): 524-529.

Qiang, L., L. Wang, N. Kon, W. Zhao, S. Lee, Y. Zhang, M. Rosenbaum, Y. Zhao, W. Gu, S. R. Farmer and D. Accili (2012). "Brown remodeling of white adipose tissue by SirT1-dependent deacetylation of Ppargamma." Cell **150**(3): 620-632.
Ratziu, V., S. A. Harrison, S. Francque, P. Bedossa, P. Lehert, L. Serfaty, M. Romero-Gomez, J. Boursier, M. Abdelmalek, S. Caldwell, J. Drenth, Q. M. Anstee, D. Hum, R. Hanf, A. Roudot, S. Megnien, B. Staels, A. Sanyal and G.-I. S. Group (2016). "Elafibranor, an Agonist of the Peroxisome Proliferator-Activated Receptor-alpha and -delta, Induces Resolution of Nonalcoholic Steatohepatitis Without Fibrosis Worsening." Gastroenterology **150**(5): 1147-1159 e1145.
Reilly, S. M. and A. R. Saltiel (2017). "Adapting to obesity with adipose tissue inflammation." Nat Rev Endocrinol **13**(11): 633-643.
Rodriguez de Fonseca, F., M. Navarro, R. Gomez, L. Escuredo, F. Nava, J. Fu, E. Murillo-Rodriguez, A. Giuffrida, J. LoVerme, S. Gaetani, S. Kathuria, C. Gall and D. Piomelli (2001). "An anorexic lipid mediator regulated by feeding." Nature **414**(6860): 209-212.
Rosen, E. D. and B. M. Spiegelman (2014). "What we talk about when we talk about fat." Cell **156**(1-2): 20-44.
Ryberg, E., N. Larsson, S. Sjogren, S. Hjorth, N. O. Hermansson, J. Leonova, T. Elebring, K. Nilsson, T. Drmota and P. J. Greasley (2007). "The orphan receptor GPR55 is a novel cannabinoid receptor." Br J Pharmacol **152**(7): 1092-1101.
Sabio, G., M. Das, A. Mora, Z. Zhang, J. Y. Jun, H. J. Ko, T. Barrett, J. K. Kim and R. J. Davis (2008). "A stress signaling pathway in adipose tissue regulates hepatic insulin resistance." Science **322**(5907): 1539-1543.
Sag, D., D. Carling, R. D. Stout and J. Suttles (2008). "Adenosine 5'-monophosphate-activated protein kinase promotes macrophage polarization to an anti-inflammatory functional phenotype." J Immunol **181**(12): 8633-8641.
Sanyal, A. J., N. Chalasani, K. V. Kowdley, A. McCullough, A. M. Diehl, N. M. Bass, B. A. Neuschwander-Tetri, J. E. Lavine, J. Tonascia, A. Unalp, M. Van Natta, J. Clark, E. M. Brunt, D. E. Kleiner, J. H. Hoofnagle, P. R. Robuck and C. R. N. Nash (2010). "Pioglitazone, vitamin E, or placebo for nonalcoholic steatohepatitis." N Engl J Med **362**(18): 1675-1685.
Sasso, O., R. Russo, S. Vitiello, G. M. Raso, G. D'Agostino, A. Iacono, G. L. Rana, M. Vallee, S. Cuzzocrea, P. V. Piazza, R. Meli and A. Calignano (2012). "Implication of allopregnanolone in the antinociceptive effect of N-palmitoylethanolamide in acute or persistent pain." Pain **153**(1): 33-41.

Saxena, N. K. and F. A. Anania (2015). "Adipocytokines and hepatic fibrosis." Trends Endocrinol Metab **26**(3): 153-161.
Schweiger, V., A. Martini, P. Bellamoli, K. Donadello, C. Schievano, G. D. Balzo, P. Sarzi-Puttini, M. Parolini and E. Polati (2019). "Ultramicronized Palmitoylethanolamide (um-PEA) as Add-on Treatment in Fibromyalgia Syndrome (FMS): Retrospective Observational Study on 407 Patients." CNS Neurol Disord Drug Targets **18**(4): 326-333.
Scuderi, C., G. Esposito, A. Blasio, M. Valenza, P. Arietti, L. Steardo, Jr., R. Carnuccio, D. De Filippis, S. Petrosino, T. Iuvone, V. Di Marzo and L. Steardo (2011). "Palmitoylethanolamide counteracts reactive astrogliosis induced by beta-amyloid peptide." J Cell Mol Med **15**(12): 2664-2674.
Scuderi, C., C. Stecca, M. Valenza, P. Ratano, M. R. Bronzuoli, S. Bartoli, L. Steardo, E. Pompili, L. Fumagalli, P. Campolongo and L. Steardo (2014). "Palmitoylethanolamide controls reactive gliosis and exerts neuroprotective functions in a rat model of Alzheimer's disease." Cell Death Dis **5**: e1419.
Seale, P., S. Kajimura, W. Yang, S. Chin, L. M. Rohas, M. Uldry, G. Tavernier, D. Langin and B. M. Spiegelman (2007). "Transcriptional control of brown fat determination by PRDM16." Cell Metab **6**(1): 38-54.
Seo, E., E. J. Park, Y. Joe, S. Kang, M. S. Kim, S. H. Hong, M. K. Park, D. K. Kim, H. Koh and H. J. Lee (2009). "Overexpression of AMPKalpha1 Ameliorates Fatty Liver in Hyperlipidemic Diabetic Rats." Korean J Physiol Pharmacol **13**(6): 449-454.
Sloan-Lancaster, J., E. Abu-Raddad, J. Polzer, J. W. Miller, J. C. Scherer, A. De Gaetano, J. K. Berg and W. H. Landschulz (2013). "Double-blind, randomized study evaluating the glycemic and anti-inflammatory effects of subcutaneous LY2189102, a neutralizing IL-1beta antibody, in patients with type 2 diabetes." Diabetes Care **36**(8): 2239-2246.
Smith, R. L., M. R. Soeters, R. C. I. Wust and R. H. Houtkooper (2018). "Metabolic Flexibility as an Adaptation to Energy Resources and Requirements in Health and Disease." Endocr Rev **39**(4): 489-517.
Spalding, K. L., E. Arner, P. O. Westermark, S. Bernard, B. A. Buchholz, O. Bergmann, L. Blomqvist, J. Hoffstedt, E. Naslund, T. Britton, H. Concha, M. Hassan, M. Ryden, J. Frisen and P. Arner (2008). "Dynamics of fat cell turnover in humans." Nature **453**(7196): 783-787.
Stern, J. H., J. M. Rutkowski and P. E. Scherer (2016). "Adiponectin, Leptin, and Fatty Acids in the Maintenance of Metabolic Homeostasis through Adipose Tissue Crosstalk." Cell Metab **23**(5): 770-784.

Suarez, J., P. Rivera, S. Arrabal, A. Crespillo, A. Serrano, E. Baixeras, F. J. Pavon, M. Cifuentes, R. Nogueiras, J. Ballesteros, C. Dieguez and F. Rodriguez de Fonseca (2014). "Oleoylethanolamide enhances beta-adrenergic-mediated thermogenesis and white-to-brown adipocyte phenotype in epididymal white adipose tissue in rat." Dis Model Mech **7**(1): 129-141.

Sugiura, T., S. Kondo, S. Kishimoto, T. Miyashita, S. Nakane, T. Kodaka, Y. Suhara, H. Takayama and K. Waku (2000). "Evidence that 2-arachidonoylglycerol but not N-palmitoylethanolamine or anandamide is the physiological ligand for the cannabinoid CB2 receptor. Comparison of the agonistic activities of various cannabinoid receptor ligands in HL-60 cells." J Biol Chem **275**(1): 605-612.

Sun, K., J. Tordjman, K. Clement and P. E. Scherer (2013). "Fibrosis and adipose tissue dysfunction." Cell Metab **18**(4): 470-477.

Takasu, T., M. Ukai, S. Sato, T. Matsui, I. Nagase, T. Maruyama, M. Sasamata, K. Miyata, H. Uchida and O. Yamaguchi (2007). "Effect of (R)-2-(2-aminothiazol-4-yl)-4'-{2-[(2-hydroxy-2-phenylethyl)amino]ethyl} acetanilide (YM178), a novel selective beta3-adrenoceptor agonist, on bladder function." J Pharmacol Exp Ther **321**(2): 642-647.

Tanaka, N., T. Aoyama, S. Kimura and F. J. Gonzalez (2017). "Targeting nuclear receptors for the treatment of fatty liver disease." Pharmacol Ther **179**: 142-157.

Theurey, P. and J. Rieusset (2017). "Mitochondria-Associated Membranes Response to Nutrient Availability and Role in Metabolic Diseases." Trends Endocrinol Metab **28**(1): 32-45.

Toda, C. and S. Diano (2014). "Mitochondrial UCP2 in the central regulation of metabolism." Best Pract Res Clin Endocrinol Metab **28**(5): 757-764.

Tsuboi, K., Y. Okamoto, N. Ikematsu, M. Inoue, Y. Shimizu, T. Uyama, J. Wang, D. G. Deutsch, M. P. Burns, N. M. Ulloa, A. Tokumura and N. Ueda (2011). "Enzymatic formation of N-acylethanolamines from N-acylethanolamine plasmalogen through N-acylphosphatidylethanolamine-hydrolyzing phospholipase D-dependent and -independent pathways." Biochim Biophys Acta **1811**(10): 565-577.

Tsuboi, K., T. Uyama, Y. Okamoto and N. Ueda (2018). "Endocannabinoids and related N-acylethanolamines: biological activities and metabolism." Inflamm Regen **38**: 28.

Tsuchida, A., T. Yamauchi, S. Takekawa, Y. Hada, Y. Ito, T. Maki and T. Kadowaki (2005). "Peroxisome proliferator-activated receptor (PPAR)alpha activation increases adiponectin receptors and reduces

obesity-related inflammation in adipose tissue: comparison of activation of PPARalpha, PPARgamma, and their combination." Diabetes **54**(12): 3358-3370.
Tutunchi, H., A. Ostadrahimi, M. Saghafi-Asl and V. Maleki (2019). "The effects of oleoylethanolamide, an endogenous PPAR-alpha agonist, on risk factors for NAFLD: A systematic review." Obes Rev **20**(7): 1057-1069.
Ueda, N., K. Tsuboi and T. Uyama (2013). "Metabolism of endocannabinoids and related N-acylethanolamines: canonical and alternative pathways." FEBS J **280**(9): 1874-1894.
Venables, B. J., C. A. Waggoner and K. D. Chapman (2005). "N-acylethanolamines in seeds of selected legumes." Phytochemistry **66**(16): 1913-1918.
Vilar-Gomez, E., Y. Martinez-Perez, L. Calzadilla-Bertot, A. Torres-Gonzalez, B. Gra-Oramas, L. Gonzalez-Fabian, S. L. Friedman, M. Diago and M. Romero-Gomez (2015). "Weight Loss Through Lifestyle Modification Significantly Reduces Features of Nonalcoholic Steatohepatitis." Gastroenterology **149**(2): 367-378 e365; quiz e314-365.
von Essen, G., E. Lindsund, B. Cannon and J. Nedergaard (2017). "Adaptive facultative diet-induced thermogenesis in wild-type but not in UCP1-ablated mice." Am J Physiol Endocrinol Metab **313**(5): E515-E527.
Wai, T. and T. Langer (2016). "Mitochondrial Dynamics and Metabolic Regulation." Trends Endocrinol Metab **27**(2): 105-117.
Wang, Q. A., C. Tao, R. K. Gupta and P. E. Scherer (2013). "Tracking adipogenesis during white adipose tissue development, expansion and regeneration." Nat Med **19**(10): 1338-1344.
Westermann, B. (2010). "Mitochondrial fusion and fission in cell life and death." Nat Rev Mol Cell Biol **11**(12): 872-884.
Wu, D., J. Liu, X. Pang, S. Wang, J. Zhao, X. Zhang and L. Feng (2014). "Palmitic acid exerts pro-inflammatory effects on vascular smooth muscle cells by inducing the expression of C-reactive protein, inducible nitric oxide synthase and tumor necrosis factor-alpha." Int J Mol Med **34**(6): 1706-1712.
Yang, Z., B. B. Kahn, H. Shi and B. Z. Xue (2010). "Macrophage alpha1 AMP-activated protein kinase (alpha1AMPK) antagonizes fatty acid-induced inflammation through SIRT1." J Biol Chem **285**(25): 19051-19059.
Zeng, W., R. M. Pirzgalska, M. M. Pereira, N. Kubasova, A. Barateiro, E. Seixas, Y. H. Lu, A. Kozlova, H. Voss, G. G. Martins, J. M. Friedman and A. I. Domingos (2015). "Sympathetic neuro-adipose connections mediate leptin-driven lipolysis." Cell **163**(1): 84-94.
Zhang, H. A., X. Y. Yang and Y. F. Xiao (2016). "AMPKalpha1 overexpression alleviates the hepatocyte model of nonalcoholic fatty liver

disease via inactivating p38MAPK pathway." Biochem Biophys Res Commun **474**(2): 364-370.
Zhu, C., C. Solorzano, S. Sahar, N. Realini, E. Fung, P. Sassone-Corsi and D. Piomelli (2011). "Proinflammatory stimuli control N-acylphosphatidylethanolamine-specific phospholipase D expression in macrophages." Mol Pharmacol **79**(4): 786-792.
Zygmunt, P. M., J. Petersson, D. A. Andersson, H. Chuang, M. Sorgard, V. Di Marzo, D. Julius and E. D. Hogestatt (1999). "Vanilloid receptors on sensory nerves mediate the vasodilator action of anandamide." Nature **400**(6743): 452-457.